

Responses to Editor and Reviewers

To:
Prof. Christine Stumpp
Editor
Hydrology and Earth System Sciences

Dear Prof. Stumpp,

We gratefully acknowledge the two reviewers for their helpful and insightful comments to improve this manuscript. We are submitting the revised manuscript titled “Application of environmental tracers for investigation of groundwater mean residence time and aquifer recharge in fault–influenced hydraulic drop alluvium aquifers” (HESS-2018-143) to ***Hydrology and Earth System Sciences***. The authors have completed revisions on the previous manuscript and have addressed a point-by-point reply to the comments below (Response in [blue](#)).

Author’s response – Line numbers referring to the old and revised version manuscripts are preceded by L and [RL](#), respectively.

Editor comments

The same two reviewers had a closer look at the revised versions. Both are experts in the research field and have different recommendations on the acceptance of the manuscript. I still see the potential that the others can revise the manuscript and that it can be a valuable contribution. It is absolutely necessary to particularly:

1) take into consideration the minor comments of reviewer #1 (see comment and attached file).

[Response: We would like to express our sincere gratitude to you for reviewing this paper. The point-by-point reply to the minor comments of reviewer #1 can be seen in “Response to **Anonymous Referee #1**”.](#)

2) do a thorough language check by a native speaker or use a public service

[Response: Agree. We have checked and revised the manuscript carefully and seriously. We also have asked a public service for help to do a thorough language check. Certificate as shown below:](#)

Certificate of Seeditors

This document certifies that the paper listed below has been edited to ensure that the language is clear and free of errors. The edit was performed by professional editors at Seeditors, a division of Delfue Communications. The intent of the author's message was not altered in any way during the editing process. The quality of the edit has been guaranteed, with the assumption that our suggested changes have been accepted and have not been further altered without the knowledge of our editors.

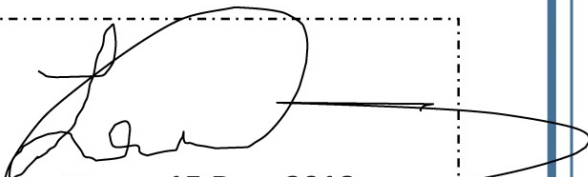
Title of the Paper

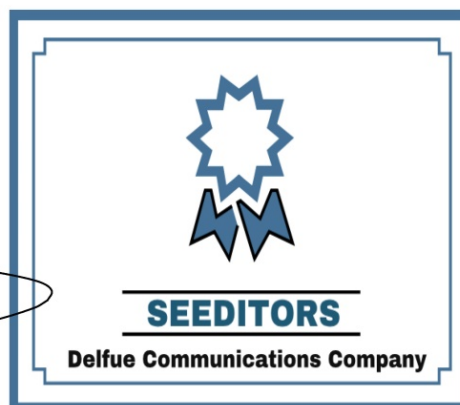
Application of environmental tracers for investigation of groundwater mean residence time and aquifer recharge in fault-influenced hydraulic drop alluvium aquifers

Ref. Number

SED01038

Signature of responsible editor:


Date of Issue : 15 Dec. 2018



Seeditors is based in the Netherlands, and has created an online workplace for the world -connecting clients with top freelance professionals and experienced small companies from Europe to North America.

Xuefeng Zhu

Dr. Xuefeng Zhu
Chief President , Seeditors

Lepelaarstraat 7, 2623NW, Delft, the Netherlands;
KVK:69163677;
T +31(0) 616828836;
E support@seeditors.com;
W www.seeditors.com.

3) go back to Maloszewski et al. 1983 and carefully check the assumptions and the physical meaning for the different functions used in the manuscript and adapt interpretation of results accordingly (see comment reviewer #2)

Response: Agree. Response can be seen in “Response to **Anonymous Referee #2**, Specific comments”.

4) consider clarification about age and apparent age.

Response: Agree. Groundwater age cannot be measured directly. Hydrogeologists use “groundwater age” to denote the time since recharge occurred or to indicate the time difference that “a water parcel needs to travel from the groundwater surface to the position where the sample is taken (i. e. *idealized groundwater age*; Suckow, 2014)”. A piston flow is premised that without mixture or non-dispersive flow along the flow paths since recharge (Cartwright et al., 2017; de Dreuz and Ginn, 2016; Suckow, 2014). However, water mixing occurs at anytime and anywhere during groundwater flow processes. The water sample taken from a well or a spring is all the time a mixture of groundwater with different ages. In our manuscript, a lumped parameter model is used to describe the distribution of residence times and at the same time to estimate the mean residence time. In Eq. (2) in the manuscript, residence time is completely equivalent to the “groundwater age” and represents the time difference (τ) between input time ($t-\tau$) and time of sampling t . Equation (2) attributes a weight ($g(\tau)$) to each of the residence times that describes to which percentage a residence time contributes to the whole mean.

$$C_{\text{out}}(t) = \int_0^{\infty} C_{\text{in}}(t-\tau) g(\tau) e^{-\lambda_{^3\text{H}}\tau} d\tau \quad \text{for } ^3\text{H} \text{ tracer} \quad (2a)$$

$$C_{\text{out}}(t) = \int_0^{\infty} C_{\text{in}}(t-\tau) g(\tau) d\tau \quad \text{for CFCs tracer} \quad (2b)$$

Since groundwater age cannot be measured directly, one can derive a groundwater age using a mathematical formula for some tracers. As the tracer concentrations (or isotope ratios, etc.) are measured based on real-world samples, the derived groundwater age is different from the residence time mentioned above. Furthermore, the age distribution in the sample is unknown, it is not possible to use Eq. (2) to estimate the mean residence time of the sample. Therefore, the widely used “apparent age” in the literatures is obtained when a mathematical formula is given and at the same time the tracer is stated. Suck (2014) emphasized that the applicable tracers to estimate the apparent ages are ^{14}C , $^3\text{H}/^3\text{He}$, ^{36}Cl , and ^{81}Kr , rather than the CFCs, SF_6 , and ^{85}Kr .

To clarify the difference between age and apparent age, statements were added in the revised manuscript for the apparent ^{14}C ages (RL213–216) and the mean residence times (RL242–250):

RL213–216: Since groundwater age cannot be measured directly, and the age distribution in the sample is unknown, one can derive an apparent age using a mathematical formula for the groundwater ^{14}C sample (Suckow, 2014). “Apparent” here describe the fact that the age is not corresponding to the time difference between recharge and sampling during which piston flow is assumed for a water parcel (Cartwright et al., 2017; Suckow, 2014).

RL242–250: A wide range of the groundwater residence times (ages) has been reported in an arid unconfined aquifer because recharge occurs under various climate conditions (Custodio et al., 2018). Furthermore, the groundwater residence time with wide variabilities that governed by the distribution of

flow paths of varying length cannot be measured directly (de Dreuz and Ginn, 2016; Suckow, 2014). A lumped parameter model may be an alternative approach to describe the distribution of residence times, which at the same time describes a mean residence time for the mixtures of different residence times. With the aid of gaseous tracers (e.g. ^3H , CFCs, SF_6 and ^{85}Kr) one can describe the distribution of tracer concentrations (Stewart et al., 2017; Zuber et al., 2005) to obtain the groundwater MRTs.

If the authors cannot consider these fundamental changes, I have to reject the manuscript.

Response: All of the comments are accepted. We have addressed all of these fundamental changes and have indicated how we will incorporate the valuable suggestions in the revised manuscript.

Anonymous Referee #1

General Comments

1) This version of the paper is better organised and clearer than the previous version. In particular, the revised Figs. 8 and 9 (now 10 and 11) are much better. Using CFC mixing model ages for interpretation (instead of the problematical CFC apparent ages) is also a big improvement. As before, I find that the paper addresses relevant scientific questions suitable for publication in HESS, with novel concepts and ideas. Substantial conclusions are reached. However, there are still problems with the English. Some suggestions for improvement in clarity are given below.

How are the mixing model calculations carried out? No information is given in the Methods Section. Are they made using the TracerLPM program of Jurgens et al. (2012)? Or have the authors developed their own program? We need to know this to assess the mixing ages.

Response: The mixing model calculation processes are as follows:

Take the CFC-12 and exponential-piston flow model (1.5) for example, the calculation process of the mean residence times is as follows: First, we chose the Eq. (2b) as the convolution integral, and chose the weighting function of the exponential-piston flow model (Eq. (3a, 3b)) as the system response function. Second, we used the time series CFC-12 trend of the Northern Hemisphere atmospheric mixing ratio (1940–2014, <http://water.usgs.gov/lab/software/air/cure/>) as input concentrations. We treated the calendar year 2015 (groundwater sampling time) as age=0 yrs by convoluting the input (times series of CFC-12 input) to the EPM (1.5). The mean residence times τ_m increased from 1 to 100 yrs with time step of 1 yr and increased from 101 to 500 yrs with time step of 5 yrs. Then we got a sequence results of output CFC-12 concentrations and mean residence times (vary from 1 to 500 yrs). Third, we plotted the output CFC-12 concentrations vs. mean residence times and then compared the measured groundwater CFC-12 concentrations to get the groundwater mean residence times. The computational procedures were carried out by using MATLAB (version R2014a). The output CFC-12 concentrations decreased from 526.4 pptv (with τ_m of 1 yr) to 3.0 pptv (with τ_m of 155 yrs). As the detection limit for each CFC is about 0.01 pmolL^{-1} of water (be equal to 3.54 pptv with the laboratory temperature of 25°C), the output CFC-12 concentrations lower than 3.54 pptv can be neglected.

2) Use of acronyms is effective (and widely practised) but should be moderate, otherwise it makes

difficulties for readers. I think MRB (Manas River Basin), MRT (mean residence time), EPM (exponential piston flow model), DM (dispersion model) and EMM (exponential mixing model) as used here are ok, but LPM and RTD should be spelled out wherever they are used (i.e. replaced by 'lumped parameter model' and 'residence time distribution').

Response: Agree and changes made. Manas River Basin (MRB), mean residence times (MRTs), exponential piston flow model (EPM), dispersion model (DM) and exponential mixing model (EMM) are used when they first appear. The abbreviations are used in the following context. "lumped parameter model" and "residence time distribution" are used throughout the manuscript.

Detailed comments

1) L44-48 This is a very muddled sentence and needs to be rewritten. Not all the radioisotopes mentioned have long half-lives. And the gases (CFCs and SF₆) are not radioisotopes, nor do they have specific half-lives.

Response: Agree and changes made (RL52–57). The sentence was revised as: Second, the atmospheric concentrations of synthetic organic compounds (chlorofluorocarbons, CFC–11, CFC–12, and CFC–113; and sulfur hexafluoride, SF₆), radioactive solute tracers such as ¹⁴C, ³⁶Cl, and noble gases (⁴He, ⁸⁵Kr, ³⁹Ar, and ⁸¹Kr), are used to determine groundwater MRTs with much wider time spans (decades to hundred millenniums; Aggarwal, 2013).

2) L75 Delete surplus "be"

Response: Agree and changes made (RL85). "be" was deleted.

3) L76 Change to ".. : for example, MRTs estimated from CFCs would be much smaller than actual values if excess air in the unsaturated zone affected CFC concentrations during recharge (Cook et al., 2006; .."

Response: Agree and changes made (RL85–89). The sentence was revised as: However, groundwater MRTs may be not always accurate based on CFCs. For example, MRTs estimated from CFCs would be underestimated if excess air in the unsaturated zone affects the CFC concentrations during recharge (Cook et al., 2006; Darling et al., 2012), or when CFC inputs are contaminated in urban and industrial environments (Carlson et al., 2011; Han et al., 2007; Mahlkecht et al., 2017; Qin et al., 2007).

4) L87 Change to "Mixing within the aquifers .. long-screened wells is expected to be common .."

Response: Agree and changes made (RL98–100). The sentence was revised as: Mixing within the aquifers and during the pumping process from the long–screened wells is expected to be common in the fault–influenced hydraulic drop alluvium aquifers of the Manas River Basin (MRB) in the arid Northwest China (Fig. 1a, b).

5) L90 Change to ".. (with water table depths of up to 180 m) .."

Response: Agree and changes made (RL101–103). The sentence was changed to: MRTs that result from a deep unsaturated zone (with water table depths of up to 180 m) and contrasting geological settings (hydraulic head drops of as much as 130 m caused by the thrust fault) are still insufficiently

recognised in the alluvium aquifer (Fig. 1c).

6) L122 Change to “.. 29 groundwater samples (pumped from fully penetrating wells, 3 springs or 3 artesian ..”

Response: Agree and changes made (RL135–137). The sentence was revised as: A total of 29 groundwater samples (pumped from fully penetrating wells, 3 springs or 3 n wells) were collected along the Manas River between June and August 2015 (from G1 to G29 in Table 1 and Fig. 2).

7) L127 “minutes” not “min”

Response: Agree and changes made (RL141). “min” was replaced by “minutes”.

8) L182 Change to “The computational ..” by omitting “Concrete”

Response: Agree and changes made (RL200). The sentence was changed to “The computational process was conducted following Plummer et al. (2006a)”.

9) L216 “although” not “despite”

Response: Agree and changes made (RL238). “despite” was changed to “although”.

10) L223 Better to spell out LPMs (i.e. lumped parameter models) here, and wherever else it occurs.

Response: Agree and changes made (RL245). “LPMs” was changed to “Lumped parameter models” and we insist on the “lumped parameter models” throughout the manuscript.

11) L245 Also RTDs (residence time distributions)

Response: Agree and changes made (RL274). “RTDs” was changed to “residence time distributions” and we insist on the “residence time distributions” throughout the manuscript.

12) L268 “compared” not “cross-referenced”

Response: Agree and changes made (RL297). “cross-referenced” was changed to “compared”.

13) L301 “.. to one or both of two recharge ..” not “.. to two recharge ..”

Response: Agree and changes made (RL331–333). The sentence was changed to: Groundwater whose isotopic values are more depleted than the modern precipitation usually would be ascribed to one or both of two recharge sources including snowmelt/precipitation at higher elevation and precipitation fallen during cooler climate.

14) L313 What do the authors mean by “qualitative recharge”? Rephrase.

Response: Agree and changes made (RL343–346). The sentence was changed to: An overlap between surface water and UG indicates the same recharge sources, because some alignment of river water and groundwater isotopic values is a qualitative indication of recharge under climate conditions similar to contemporary conditions (Huang et al., 2017).

15) L389 Use “but not” instead of “rather than”

Response: Agree and changes made (RL428). “rather than” was changed to “but not”.

16) L403 “groundwater is mainly recharged by fast river leakage” not “groundwater mainly recharged

by the river fast leakage”

Response: Agree and changes made (RL440–442). The sentence was revised as: Studies on the MRB (Ma et al., 2018; Wang, 2007; Zhou, 1992) have shown that groundwater is mainly recharged by fast river leakage in the upstream area and piedmont plain, where the soil texture consists of pebbles and sandy gravel (Fig. 1c).

17) L414 Add words. “indicated input of some fractions” not “indicated some fractions”

Response: Agree and changes made (RL450–451). The sentence was changed to: All of the ^3H values in UG (G1, G2, and G4) and G23 (belonging to MG) are higher than 34.3 TU, which indicate input of some fractions of the 1960s precipitation recharge.

18) L462-464 Unclear sentence. “But river leakage and rainfall input could have come only from the piedmont plain (Ma et al., 2018), thus a smaller proportion of piston flow in the EPM could give an EPM ratio of 2.2 (I_E in Eq. (3) would only be for the piedmont plain in Fig. 1c).” not “River leakage and rainfall input were possible from the piedmont plain (Ma et al., 2018), thus a less proportion of piston flow by the EPM with an EPM ratio of 2.2 (I_E in Eq. (3) is only in the piedmont plain in Fig. 1c) was also used.”

Response: Agree and changes made (RL502–505). The sentence was revised as: But the river leakage and rainfall input could have come only from the piedmont plain (Ma et al., 2018), thus a smaller proportion of piston flow in the EPM could give an EPM ratio of 2.2 (I_E in Eq. (3) would only be for the piedmont plain in Fig. 1c).

19) L499-500 Unclear sentence. “Nevertheless, the homogeneous aquifers, being at steady–state, justify the use of LPMs to calculate MRTs in this study.” Not “Nevertheless, in this study the homogeneous aquifers, being at steady–state, justifying the use of LPMs to calculate MRTs.”

Response: Agree and changes made (RL557–559). The sentence was revised as: Nevertheless, the homogeneous aquifers, being at steady–state, justify the use of lumped parameter models to calculate MRTs in this study.

20) L503 “closed” not “close”

Response: Changes made (RL563). “close” was changed to “similar”.

21) L504 “better” not “higher”

Response: Agree and changes made (RL564). “higher” was replaced by “better”.

22) L519 “MRT” not “MTT”

Response: Agree and changes made (RL579). “MTT” was changed to “MRT”.

23) L539 “On the other hand” not “However”

Response: Agree and changes made (RL599). “However” was replaced by “On the other hand”.

24) L552 “and different young water inputs in different decades” not “and young water mixtures in different decades”

Response: Agree and changes made (RL617–619). The sentence was revised as: Furthermore, the mixing diversity is highlighted by the substantial water table fluctuations during groundwater pumping,

vertical recharge through the thick unsaturated zone, and different young water inputs in different decades.

25) Table 1 caption. Change order to match the columns in the table. “.. stable isotopes, CFCs, tritium ..”

Response: Agree and changes made (RL814). Table 1 caption was revised as: **Table 1.** Chemical–physical parameters, stable isotopes, CFC concentrations, tritium (^3H), and ^{14}C in groundwater samples in the Manas River Basin.

26) Table 2 caption. Change order to match columns and add words at end. “.. partial pressure (pptv), fraction of post-1940 water, modern precipitation recharge year, and mean residence times based on different lumped parameter models (EPM, DM and EMM).”

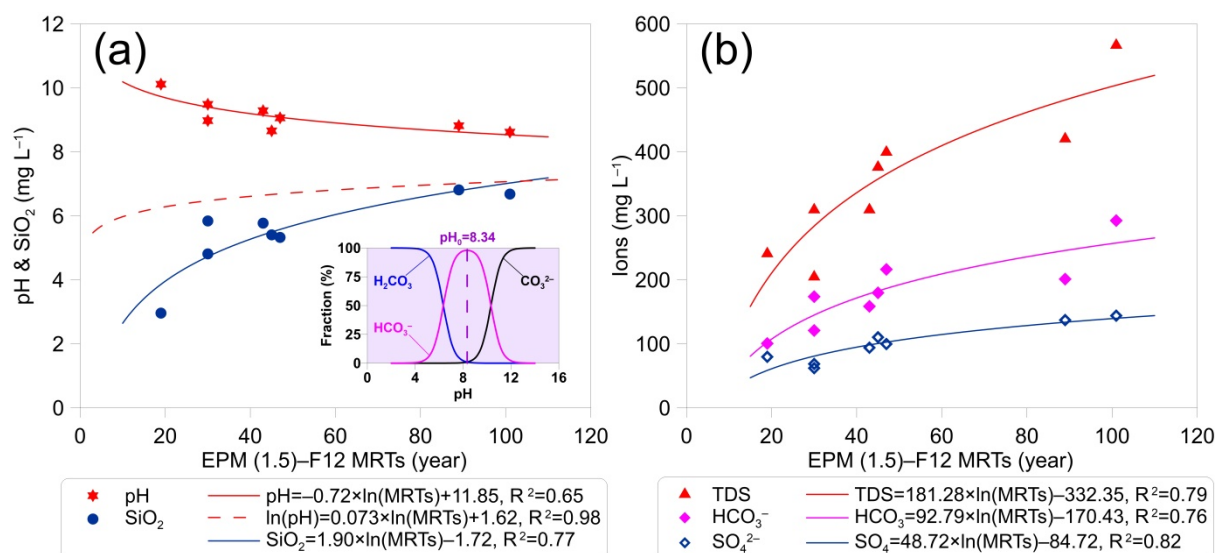
Response: Agree and changes made (RL816). Table 2 caption was revised as: **Table 2.** Calculated results for CFC atmospheric partial pressure (pptv), fraction of post–1940 water, modern precipitation recharge year, and mean residence times (EPM, DM and EMM).

27) Figure 11 caption has too much jargon. Change to “(a) Mean residence times (MRTs) for CFC-12 vs. MRTs for CFC-11 and CFC-113 data using the EPM (1.5) model. (b) MRTs for CFC-12 with EPM (1.5) vs. those with other models. (c) MRTs for ^3H vs. those with other models.

Response: Agree and changes made (RL878). Figure 11 caption was revised as: **Figure 11.** (a) Mean residence times (MRTs) for CFC–12 vs. MRTs for CFC–11 and CFC–113 data using the EPM (1.5) model. (b) MRTs for CFC–12 with EPM (1.5) vs. those with other models. (c) MRTs for ^3H vs. those with other models.

28) Figure 12(a) and (b) The x-axes should have “MRT” not “MTT”.

Response: Agree and changes made (RL885). Figure 12 was revised as:



29) Figure 12 caption. Change to “(a) pH and silica (SiO₂) and (b) sulfate (SO₄), bicarbonate (HCO₃), and total dissolved solids (TDS) vs. mean residence times (MRTs). The MRTs are from CFC-12 data using the EPM (1.5) model. The dashed red line ..”

Response: Agree and changes made (RL888). Figure 12 caption was revised as: **Figure 12.** (a) pH and silica (SiO_2) and (b) sulfate (SO_4^{2-}), bicarbonate (HCO_3^-), and total dissolved solids (TDS) vs. mean residence times (MRTs). The MRTs are from CFC-12 data using the EPM (1.5) model. The dashed red line in (a) is from Morgenstern et al. (2015).

Anonymous Referee #2

General Comments

The authors have obviously taken great pain to respond to the reviewers' criticisms constructively. They have failed completely however to address the fundamental issues raised by the reviewers. Changes are numerous and quite substantial, but superficial. Hence, I still stand to my initial assessment that the authors have written a relatively well done case study that however falls completely short of any kind of originality or innovativeness. The manuscript imitates previous works, but even in what the authors have shown of the revised version, it still suffers from its lack of focus. Estimating groundwater residence times from multiple tracers has been done and redone so many times and is not a sufficient reason for a publication in HESS, except if a methodological breakthrough of sorts can be presented (this is not at all the case here).

Furthermore, the authors are STILL inconsistent in the use they make of the weighting functions, presenting three potential models (EPM, EMM and DM) in the method section, but retaining the piston-flow model for the analysis of the carbon 14 data. If anything, this shows that the authors have not fundamentally modified their initial (erroneous) analysis, although prompted to do so by the reviewers.

Response: We sincerely thank you for taking the time to review our manuscript and for your insightful comments. We think that it is not contradictory to estimate groundwater mean residence time using a lumped parameter model with different weighting functions and to determine groundwater ^{14}C apparent age using a mathematical formula. As shown in the "Response to Editor comments 4", apparent age is derived from the ^{14}C tracer. Because the apparent ^{14}C age is derived from a real-world sample, in which the age distribution in the sample is unknown and the sample is an aggregation of many piston flow lines of water. We treated the apparent ^{14}C ages with caution. Therefore, we did not compare the apparent ^{14}C ages with mean residence times that derived from a lumped parameter model with different weighting functions (EPM, EMM, and DM). Furthermore, in the revised manuscript, groundwater ^{14}C activity is used to help to investigate groundwater recharge features (i.e. the modern and paleo-meteoric recharge features).

Specific comments

1) Remark 3: One can always argue that any kind of environmental or hydrological study is "essential" because of human induced pressures, climate change, necessity to provide policy support data, etc... What I meant to say was however much more simply that I do not see anything new or innovative in the manuscript. I still do not. In particular, the authors reproduce the overall shortcomings of many recent publications on multi-tracer groundwater studies, where the multiple tracer measurements are not used to derive one of more consistent parameterised models (see Maloszewski et al., Journal of Hydrology 66, 1983 for a good example), but instead juggle more or less successfully between differ-

ent estimates of the mean transit time obtained from each tracer, sometimes comparing the results of models assuming incompatible weighting functions.

Response: Both the study by Małoszewski et al. (1983) and many recent studies (i.e. Cartwright and Morgenstern, 2015, 2016; Cartwright et al., 2018; Han et al., 2015; Morgenstern and Daughney, 2012; Morgenstern et al., 2015) have determined groundwater mean residence time (or mean transit time) using a lumped parameter model. The mean residence times were determined based on different response functions (EPM, EMM, and DM) that describe the residence time distributions. In fact, the earlier study by Małoszewski and Zuber (1982, 1996), as well as the studies in recent years (i.e. Jurgens et al., 2012), have systematically summarized possible applicability of particular models (like piston flow model, exponential mixing model, exponential–piston flow model, dispersion model, etc.) in the different subsurface flow systems. The fact is that lumped parameter model premises that the idealized flow system is at a steady state, which differs from the actual hydrogeological conditions. Integrated application of the different response functions mentioned above is reasonably to determine groundwater mean residence time. Małoszewski et al. (1983) pointed out that “*applications are limited to the frequently used exponential (EM) and dispersive model (DM)*” in their paper. Recent studies by Cartwright and Morgenstern (2015, 2016) compared the mean residence times determined from different models (EPM, EMM, and DM). Morgenstern et al. (2010) obtained an excellent correlation between silica (SiO_2) and mean residence time ($R^2=0.997$) in their paper, where an exponential–piston flow model with an exponential fraction of 80% was used (rather than the exponential fraction of 70% and 90%). Examples mentioned above help us to get a more comprehensive understanding of the mean residence time in a hydrological system by comparing the different models. In our manuscript, exponential–piston flow model, exponential mixing model, and dispersion model were used because these three models are all possible applicability for the hydrological systems in the Manas River Basin. We believe that the response functions used in our manuscript (EPM, EMM, and DM) are considered carefully and that the corresponding mean residence times are proper to be explained.

2) Remark 4: “The groundwater residence times (ages) often display a wide range due to the recharge under various climate conditions”. This is correct, but only in a very particular case of arid to hyperarid environments having known a wetter period. In temperate climates, the distribution of transit time at the outlet of a groundwater system is due to the differences in length and flow time of the flow tubes contributing to discharge.

Response: Agree and changes made. The sentence was changed to (RL242–245): A wide range of the groundwater residence times (ages) has been reported in an arid unconfined aquifer because recharge occurs under various climate conditions (Custodio et al., 2018). Furthermore, the groundwater residence time with wide variabilities that governed by the distribution of flow paths of varying length cannot be measured directly (de Dreuz and Ginn, 2016; Suckow, 2014).

As we know that residence time varies both temporally following hydrological fluctuations and spatially following geological settings. Also, topographic and geomorphic conditions as well as evaporation intensity will influence the residence time. Custodio et al. (2018) reported a typical research on the residence time with wide ranges in a large unconfined aquifer, in which a wet period intercalated in an arid climate sequence having known. Furthermore, factors that change the groundwater flow paths may lead to variation of the residence time.

Remark 4: “The exponential–piston flow model (EPM) describes aquifer that containing a segment of

exponential flow followed by a segment of piston flow. Piston flow assumes that water mixing from different flow lines is minimal and receiving little or no recharge in the confined aquifer, and the exponential flow assume a full mixing of water in the unconfined aquifer and receiving areally distributed recharge". This description is not correct, and confirms my impression that the authors do not quite know what they are doing. The EPM does not prescribe the order in which the two components are physically arranged (this is explicitly explained in Maloszewski and Zuber, 1983), because mathematically, it makes no difference for the output concentration. And as far as the exponential model is concerned, mixing occurs at the sampling point and is only exactly true for semi-confined aquifers (see Haitjema, Journal of Hydrolog 172, 1995).

Response: The statement "The exponential–piston flow model (EPM) describes aquifer that containing a segment of exponential flow followed by a segment of piston flow" is used to describe the particular model (i.e. exponential–piston flow model), which shows us an imagination of the schematic diagram of the idealized aquifer configuration (Jurgens et al., 2012; Małoszewski and Zuber, 1982, 1996). In general, a groundwater flow pattern that unconfined aquifer receives vertical water recharge following confined aquifer without vertical water recharge is the most common from mountain to plain in the arid areas. Furthermore, mixing may occur both in the long screened well and at the sampling point for the exponential model, and it is also true for the unconfined aquifers (Jurgens et al., 2012; Małoszewski and Zuber, 1982, 1996).

Remark 4: "the MRTs with different RTDs were cross–referenced". What does that mean? Comparing the estimated mean transit times really leads nowhere. Either they are close and the authors will claim there is "satisfactory agreement", or they are not and an entire section of the discussion will be devoted to that. Model choice still is an open research question, so either the authors present a solid argument as to which model they chose, or some kind of methodology allowing to reject some models (as flawed as it is, the method by Plummer et al. is one example of that).

Response: Model choice should be based on the subsurface water flow system pattern as well as the hydrogeology setting. It is seen from Fig. 1 that the subsurface water flow system is controlled by the hydrogeological conditions and the geological settings (i.e. the thrust fault with block water feature). Aquifer recharge is mainly from the lateral flow in the mountain area as well as the fast river leakage in the intermountain depression and in the piedmont plain. Moreover, the river leakage occurs mainly along the river flow motion with small areas. Vertical recharge from the precipitation in the intermountain depression and in the piedmont plain is rare, and is little and even is none in the oasis plain in the arid Manas River Basin. Hence, there is not an exact idealized aquifer configuration (Jurgens et al., 2012; Małoszewski and Zuber, 1982, 1996) to be applied to groundwater samples in our study area. What we tend to do is comparing the mean residence times determined from different idealized models. It is also a choice to do so in other study areas (e.g. Cartwright and Morgenstern, 2015, 2016).

Remark 4: "In our manuscript, the apparent ^{14}C ages estimation was adopted." I have already criticised this in the first review. "Apparent age" means you are assuming a piston-flow weighting function. This is not consistent with the method section presenting the EPM, the DM and the EMM as potential models describing the transit time distribution of the aquifer.

Response: Partly agree. In the revised manuscript, we added statement for the term "apparent age". The clarification for "Apparent ^{14}C ages" is seen in the "Response to editor comment 4". Apparent ^{14}C age is determined from a real-world sample using a defined formula (Eq. 1 in the manuscript). As the

distribution function for the residence times is unknown in the sample, it represents an unknown average of the residence times.

3) Remark 50: “We think that combining ^3H and CFCs is a good tool to distinguish the modern precipitation recharge and to indicate the groundwater mixing properties”. I do not quite know what the authors mean by groundwater mixing properties, but the rest of the paragraph is not an answer to my point at all concerning the very limited use of binary mixing diagrams in multi-tracers studies. The authors just equivocate without actually trying to propose a counter argument.

Response: In the revised manuscript, diagram of ^3H vs. CFCs helps to investigate recharge features due to the large difference of the temporal pattern in the input functions between CFCs and ^3H . Compared with plots of tracer ratios, tracer–tracer concentration plots have some advantages because they reflect more directly the measured quantities and potential mixtures, such as mixing with irrigation water or young water mixtures in different decades (RL466–480).

4) Remark 57: Figure 11 has been kept by the authors, who at the same time have deleted references to “apparent age” from their manuscript, but not from the analysis! Do they realize that the plots of figure 11, being calculated using a piston-flow model, show this very “apparent age” they agreed makes no sense?

Response: In the revised manuscript, Figure 11 (It is Fig. 7 in the revised manuscript) helps to identify samples containing young (post–1940) and old (CFC–free) water or exhibiting contamination or degradation. The young water fractions are also determined using the binary mixing method. It is nothing to do with “apparent age” in Fig. 7 in the revised manuscript.

Application of environmental tracers for investigation of groundwater mean residence time and aquifer recharge in ~~faulted~~-fault-influenced hydraulic drop alluvium aquifers

5 Bin Ma^{1,2}, Menggui Jin^{1,2,3}, Xing Liang^{1,4}, and Jing Li¹

¹School of Environmental Studies, China University of Geosciences, Wuhan, 430074, China

²State Key Laboratory of Biogeology and Environmental Geology, China University of Geosciences, Wuhan, 430074, China

³Laboratory of Basin Hydrology and Wetland Eco-restoration, China University of Geosciences, Wuhan, 430074, China

10 ⁴Hubei Key Laboratory of Wetland Evolution & Ecological Restoration, China University of Geosciences, Wuhan, 430074, China

Correspondence to: Menggui Jin (mgjin@cug.edu.cn)

Abstract. ~~Documenting- Investigating~~ groundwater residence time and ~~the~~ recharge source is crucial for water resource management in the alluvium aquifers of arid basins. Environmental tracers (CFCs, ³H, ¹⁴C, $\delta^2\text{H}$, $\delta^{18}\text{O}$) and groundwater hydrochemical components are used for assessing groundwater mean residence times (MRTs) and aquifer recharge in ~~faulted~~-fault-influenced hydraulic drop alluvium aquifers in the Manas River Basin (China). Aquifers under the Manas River upstream (south of the fault) containsThe very high ³H activity (41.1–60 TU), in the groundwater in the Manas River upstream (south of the fault) indicates rainfall recharge duringimplying water recharge affected by the nuclear bomb tests (since of the 1960s). Carbon-14 groundwater age increases withpositively correlated with distance from mountain area (3000–5000 yrs in the midstream to > 7000 yrs in the downstream) and groundwater depth, as well as but negatively correlates to with decreasingdecrease of ³H activity (1.1 TU) and more negative $\delta^{18}\text{O}$ values, confirming-This phenomenon reveals that the source of the deeper groundwater in the semi-confined aquifer is ~~derived from~~ paleometeoric recharge in the semi-confined groundwater system. Special attention has been paid to the estimation of MRTs ~~estimated~~-using CFCs and ³H by an exponential-piston flow model. The results show that MRTs vary from 19 to 101 yrs ~~for by~~ CFCs and from 19 to 158 yrs ~~for by~~ ³H; MRTs ~~for estimated from~~ ³H are much longer than those ~~for from~~ CFCs, probably due to the different time lag of (liquid (³H) ~~vs. and~~ gas phase) (CFCs) through the ~~thick~~-unsaturated zone. The MRTs estimated by CFCs show good remarkable correlations between CFCs rather than ³H MRTs and with pH; and the concentrations of SiO₂; and SO₄²⁻, which can provide a concentrations allow estimating possible approach to estimate first-order proxies of MRTs for groundwater age at different times. The young water fractions are investigated by the CFC binary mixing method in the south and north of the fault. Relatively modern recharge is found in the south of the fault with young (post-1940) water fractions of 87–100 %, whereas in the north of the fault ~~in the midstream area~~ the young, water fractions vary from 12 to 91 % ~~based on the CFC binary mixing method~~. This study shows that the combination of CFCs and ³H residence time tracers can help analyse the groundwater MRTs and identify the recharge sources for the different mixing end-members.

1 Introduction

Groundwater is the ~~world's~~ largest available freshwater resource. ~~It~~ supplies freshwater to ~~billions of people communities~~ around the world, and ~~it~~ plays an essential central role in energy and food security, human health, and ecosystems conservation (Gleeson et al., 2016). ~~Documenting- Investigating~~ the residence time of groundwater (i.e. ~~time- the period~~ from recharge to drainage in pumping wells, springs, or streams) reveals information about water storage, mixing, and transport in subsurface water systems (Cartwright et al., 2017; Dreuzy and Ginn, 2016; McGuire and McDonnell, 2006). This is particularly crucial- important in alluvium aquifers where fresh groundwater renewability is generally strong (Huang et al., 2017), thus functioning as potable water resources in ~~the~~ arid areas; ~~also~~. Moreover, alluvium aquifers are more- increasingly vulnerable to anthropogenic contaminants and land-use changes (Morgenstern and Daughney, 2012).

Because the residence time distribution in subsurface water systems cannot be empirically measured, a commonly used approach is parametric fitting of trial distributions to chemical concentrations (Leray et al., 2016; Suckow, 2014). The widely used lumped- parameter models (~~LPMs~~; Małozzewski and Zuber, 1982; Jurgens et al., 2012), which commonly assume that the hydrologic system is at a steady- state, have been applied to subsurface water systems (Cartwright et al., 2018; McGuire et al., 2005; Morgenstern et al., 2015; Stewart et al., 2010). ~~containing young water with modern tracers of variable input concentrations (e.g. seasonably variable stable isotope ^2H and ^{18}O , tritium, and ^{85}Kr ; Cartwright et al., 2018; McGuire et al., 2005; Morgenstern et al., 2015; Stewart et al., 2010)~~. The groundwater residence time tracers can be classified into three types depending on ~~their- the~~ time span they measure. ~~The F~~ First, isotopes of water (^{18}O , ^2H , ^3H), are ideal tracers for determining ~~the~~ mean residence times (MRTs) shorter than approximately 5 yrs with stable isotopes (Kirchner et al., 2010; McGuire et al., 2005; Stewart et al., 2010) and up to approximately 100 yrs with ^3H (Beyer et al., 2016; Cartwright and Morgenstern, 2015, 2016; Morgenstern et al., 2010). Second, the atmospheric concentrations of synthetic organic compounds (chlorofluorocarbons, CFC-11, CFC-12, and CFC-113; and sulfur hexafluoride, SF_6), radioactive solute tracers such as ^{14}C , ^{36}Cl , and noble gases (^4He , ^{85}Kr , ^{39}Ar , and ^{81}Kr), ~~as well as the atmospheric concentrations of synthetic organic compounds (chlorofluorocarbons, CFC-11, CFC-12, and CFC-113; and sulfur hexafluoride, SF_6)~~, are used in determining to determine groundwater MRTs with a-much wider time spans (decades to hundred millenniums) ~~due to the radioisotopes long half- lives (-~~; Aggarwal, 2013). ~~The F~~ Third, concentrations of major ions such as inert chloride (Cl) ~~ions~~ determine MRTs in a similar way to ~~the~~ stable isotopes depending on the damping of seasonal variation input cycles that pass through a system into the output. MRTs determined through the seasonal tracer cycle method (e.g., stable isotope values or Cl concentrations), which requires detailed time series measurements, such as weekly or more frequent time steps, may be more appropriate for water drainage through a catchment and discharging into a stream (Hrachowitz et al., 2009; Kirchner et al., 2010; McGuire et al., 2005) ~~than for a groundwater system~~. Nevertheless, a strong correlation of major ion concentrations with groundwater age enables hydrochemistry to be used as proxy for age or complementary to age via previously established relationships in closed lithological conditions (Beyer et al., 2016; Morgenstern et al., 2010, 2015).

65 The ~~only~~-true age ~~for-of~~ water ~~is-can only be determined through~~ ^3H , a component of the water molecule with a half-life of 12.32 yrs (Tadros et al., 2014). ~~The Northern Hemisphere~~- ^3H activity ~~in the Northern Hemisphere~~ is several orders of magnitude higher than that in the Southern Hemisphere (Clark and Fritz, 1997; Tadros et al., 2014) due to the atmospheric thermonuclear tests ~~in the Northern Hemisphere~~ in 1950s and 1960s; which resulted in mean annual ^3H activity peaks reaching several hundred times ~~that of the~~-natural levels ~~in the Northern Hemisphere~~. The present-day rainfall ^3H activity in 70 the Northern Hemisphere is still affected by the tail-end of the bomb-pulse, ~~and it is~~-particularly high ~~in the arid regions of~~ Northwest China due to both the continental effect (Tadros et al., 2014) and the China atmospheric nuclear tests from 1964 to 1974. Thus, measurement of a single sample of ^3H activity does not accurately assess the groundwater MRTs in the Northern Hemisphere (Cook et al., 2017), and time-series ~~of~~ ^3H measurements with ~~LPMs-lumped parameter models~~ are required (Han et al., 2007; Han et al., 2015).

75 In contrast to ^3H , CFCs degrade slowly in the atmosphere and have ~~relatively-longer~~ degradation half-lives, which permits their uniform atmospheric distributions over large areas; ~~H~~however, there is 1–2 yrs lag for the Southern Hemisphere compared with the Northern Hemisphere (Cartwright et al., 2017; Cook et al., 2017; Darling et al., 2012). The build-up of CFCs in the atmosphere after the 1950s coupled with their solubility ~~in water~~ (despite low solubility) ~~in-water~~ enables them to be commonly used as indicators of groundwater MRTs up to approximately 60 yrs (Darling et al., 2012; Han et al., 2012). 80 Although the atmospheric concentrations of CFC-11, CFC-12, and CFC-113 ~~have~~-declined between 1994 and 2002 (different CFCs peaked at different times; Cook et al., 2017), thereby leaving room for ambiguity in the CFC ratio plots (Darling et al., 2012), the different atmospheric CFC ratios between today and pre-1990s (Plummer et al., 2006b) enable determination of groundwater MRTs using CFCs. Consequently, CFCs have been commonly viewed as ~~an~~ alternatives to ^3H for calculating groundwater MRTs ~~with-following~~ the decline in the bomb-pulse ^3H activity (Cartwright et al., 2017; Cook et al., 2017; Qin et al., 2011). However, groundwater MRTs may ~~be~~ not ~~be~~-always ~~be~~-accurate ~~when-calculated-usingbased~~ 85 ~~on-CFCs~~; ~~F~~for example, MRTs ~~estimated from CFCs would be~~ ~~are-much-lower-than-the-actual-values~~ ~~underestimated~~ if ~~excess air in the unsaturated zone affects the~~ CFC concentrations ~~inputs-are-entrapped-excess air in the unsaturated zone~~ during recharge (Cook et al., 2006; Darling et al., 2012), ~~or when CFC inputs are contaminated or contaminated~~ in urban and industrial environments (Carlson et al., 2011; Han et al., 2007; Mahlknecht et al., 2017; Qin et al., 2007); ~~and-On the other~~ 90 ~~hand, groundwater MRTs would be overestimated~~ ~~are-much-higher~~ if CFC inputs are degraded in anaerobic groundwater (most notably CFC-11 and CFC-113; Cook and Solomon, 1995; Horneman et al., 2008; Plummer et al., 2006b).

Additionally, mixing between water of different ages, which occurs ~~both~~-within the aquifer ~~and-or during~~ pumping from long-screened wells (Cook et al., 2017; Custodio et al., 2018; Visser et al., 2013), poses difficulties for estimating- MRTs using tracer data. The calculated MRTs will be less than the actual values in ~~the~~ mixed water due to aggregation errors 95 (Cartwright and Morgenstern, 2016; Kirchner, 2016; Stewart et al., 2017). MRTs estimation using a multi-model approach based on incorporated residence time tracers ~~should-would~~ reduce the calculation uncertainty (Green et al., 2016; Visser et al., 2013) and indicate whether MRTs can be realistically estimated (Cartwright et al., 2017).

~~The hypothesis is~~ Mixing within the aquifers and during the pumping process from the long-screened wells is expected to be common in the faulted-fault-influenced hydraulic drop alluvium aquifers of the Manas River Basin (MRB) in the arid ~~regions of~~ Northwest China (Fig. 1a, b). In particular, pumping from long-screened wells (of which there are over 10 000 boreholes, Ma et al., 2018) makes groundwater mixing most likely to occur. MRTs that result from a deep unsaturated zone (with ~~a~~-water table depths of up to 180 m) and contrasting geological settings (~~a level difference of 130 m~~ hydraulic head drops of as much as 130 m caused by the thrust fault) are still insufficiently recognised in the alluvium aquifer (Fig. 1c). We aim to provide the first estimation of ~~the~~ MRTs ~~of from~~ borehole groundwater drainage (e.g., well withdrawal) using CFCs and ³H-~~concentrations~~. We will then analyse the major hydrochemical ions in groundwater as first-order proxies for MRTs. In addition, we identify the recharge sources for the different mixing end-members and constrain mixing rates.

2 Geological and hydrogeological setting

The bedrock of the upper Manas River catchment in the mountain area of Northwest China consists of granites, sedimentary formations of Devonian and Carboniferous age, and Mesozoic limestone (Jelinowska et al. 1995). Pyroclastic rock is exposed in relatively small areas in the south mountain. The piedmont and oasis plains are ~~filled with~~within the Cenozoic strata, including ~~the~~ Tertiary and Quaternary deposits with a total depth of more than 5000 m in the piedmont area and ~~decreasing to~~ 500–1000 m in the centre of the plain (Zhao 2010). The vertical cross section (Fig. 1c) shows that the Quaternary deposits consist of pebbles, sandy gravel, and sand in the piedmont plain. The clay content in the Quaternary deposits increases from the overflow spring zone to the north oasis plain, which consists of silty loam and clay. The Huoerguosi–Manas–Tugulu thrust faults occurred in the early Pleistocene and cut the Tertiary strata with a total length of approximately 100 km in the piedmont alluvial fan (Fig. 1); ~~which these~~ are water block features. These faults were intermittently active ~~from in~~ the middle late–Pleistocene and then ~~tended to be~~were more active from the late Holocene (Cui et al., 2007).

In the mountain area, groundwater consists of metamorphic rock fissure water, magmatic rock fissure water, clastic rock fissure water, and Tertiary clastic rock fissure water (Cui et al., 2007; Zhou, 1992). In the piedmont plain of the Shihezi (SHZ) zone, groundwater is from a single-layer unconfined aquifer. From the overflow spring zone to the central oasis plain, groundwater consists of shallow unconfined water and deep confined water. The hydraulic gradient, hydraulic conductivity, and transmissivity show a large range of variations due to changes in grain size and local increases of clay content (Wu 2007). The groundwater flow direction is consistent with the Manas River flow direction. In the piedmont plain, the unconfined aquifer with saturated thickness more than 650 m is recharged by the Manas River water ~~and unconfined with saturated thickness more than 650 m~~, and is hydraulically connected to the hydrological network in the piedmont plain and north oasis plain (Ma et al., 2018; Wu 2007). The depth of the piedmont plain unconfined aquifer ~~depth~~ decreases gradually from south to north and has relatively fresh groundwater with TDS of < 1 g L⁻¹. Groundwater discharges via springs in the northern area of SHZ (Fig. 1c). Groundwater in the ~~The~~ shallow unconfined groundwater aquifer in the north oasis plain has

130 TDS of $> 3 \text{ g L}^{-1}$, and the TDS of groundwater in the underlying confined groundwater aquifer show relatively fresh water
with TDS of varies from $0.3\text{--}1.0 \text{ g L}^{-1}$ (Wu 2007). The water table depth is as deep as 180 m and a level difference of 130
m the hydraulic head drops as much as 130 m is observed due to the thrust fault in the south margin in SHZ (Fig. 1c).

3 Materials and methods

3.1 Water sampling

135 ~~In A total, of~~ 29 groundwater samples (pumped from fully penetrating wells, ~~of which 3 are from spring and 3 are from the~~
artesian wells) were collected along the Manas River ~~during between~~ June ~~to and~~ August, 2015 (from G1 to G29 in Table 1
and Fig. 2). Groundwater Locations were separated into three clusters based on the hydrochemistry and stable isotope data:
~~including~~ the upstream groundwater (UG, south of the Wuyi Road), midstream groundwater (MG, area between the Wuyi
140 Road and the West Main Canal–Yisiqi), and downstream groundwater (north of the West Main Canal–Yisiqi) ~~based on the~~
hydrochemistry and stable isotope data. Groundwater ~~were was~~ sampled from wells for irrigation and domestic supply, in
which shallow wells were pumped for a minimum of 5 min minutes before sampling and deep wells were active for
irrigation for more than 10 days prior to ~~the~~ sampling. Surface water samples data (river water, ditch and reservoir water)
and groundwater samples data (sample ID are from G30 to G39) ~~data from G30 to G39~~ were reported by Ji (2016) and Ma et
al. (2018).

145 Water temperature (T), pH ~~values~~, electrical conductivity (EC), and dissolved oxygen (DO) were measured (Table 1) in
the field using calibrated Hach (HQ40d) conductivity and pH meters, which had been calibrated before use. Bicarbonate was
determined by titration with 0.05 N HCl on site. Samples to be ~~analyzed~~ analysed for chemical and stable isotopic values
were filtered on site through $0.45 \mu\text{m}$ millipore syringe filters and stored in pre-cleaned polypropylene bottles at $4 \text{ }^{\circ}\text{C}$ until
analysis. For cation and strontium isotope analysis, the samples were acidified to $\text{pH} < 2$ with ultrapure HNO_3 .

150 For CFCs samples ~~Extreme precautions are needed to beware~~ taken to avoid contamination from equipment such as
pumps and tubing (Cook et al., 2017; Darling et al., 2012; Han et al., 2012) ~~for CFCs samples~~. After purging the wells, ~~the~~
water samples were collected directly from the borehole using a copper tube sampling pipe ~~for CFC analysis~~. One end of the
pipe was connected to the well casing, and the other end was placed in the bottom of a 120 mL borosilicate glass bottle,
inside a 2000 mL beaker. The well water was allowed to flow through the tubing for ten minutes, thoroughly flushing the
155 tubing ~~with well water~~. The bottle was submerged, and then filled and capped underwater when ~~there was~~ no bubbles
appeared in the bottle, following the protocols described by Han et al. (2007). In this study, 5 bottles were collected at each
well, ~~and~~ 3 of which were ~~analyzed~~ analysed. A total of 10 wells were collected for CFCs analysis (CFC–11, CFC–12 and
CFC–113) ~~analysis~~. Unfiltered groundwater samples for ^3H analysis were collected and stored in 500 mL airtight
polypropylene bottles. Dissolved inorganic carbon (DIC) for ^{14}C activity analysis was precipitated to BaCO_3 and sealed in
160 500 mL polypropylene bottles in the field from 180 to 240 L water samples ~~to BaCO_3~~ following the procedure reported by

~~Chen et al. (2003). This was done by the addition of excess BaCl₂ previously brought to pH ≥ 12 by addition of with NaOH, which then were sealed in 500 mL polypropylene bottles, following the procedure reported by Chen et al. (2003).~~

3.2 Analytical techniques

The CFC concentrations were analysed within 1 month of sample collection at the Groundwater Dating Laboratory of the
165 Institute of Geology and Geophysics, Chinese Academy of Sciences (IGG-CAS) using a purge-and trap gas chromatography procedure with an Electron Capture Detector (ECD), ~~which~~ The procedure has been reported by Han et al. (2012, 2015) and Qin et al. (2011). ~~The procedures were, which is modified after by from~~ Oster et al. (1996). The detection limit for each CFC is about 0.01 pmol L⁻¹ of water, with ~~the an error~~ less than ±5 %. The obtained results are shown in Table 1.

170 The ³H and ¹⁴C activities of groundwater were measured using liquid scintillation spectrometry (1220 Quantulus ultra-low-level counters, PerkinElmer, Waltham, MA, USA) at the State Key Laboratory of Biogeology and Environmental Geology, China University of Geosciences in Wuhan. Water samples for ³H were distilled and electrolytically enriched prior to being analysed. Detailed procedures were after by Morgenstern and Taylor (2009). ³H activities were expressed as tritium unit (TU), with 1 TU corresponding to a ³H/¹H ratio of 1 × 10⁻¹⁸. For ¹⁴C samples, the obtained BaCO₃ samples were first
175 converted to CO₂, then to acetylene (C₂H₂) which in turn was trimerized catalytically to C₆H₆ as described by Polach (1987), prior to being analysed. ¹⁴C activities were reported as percent modern carbon (pMC). The achieved precision for ³H and ¹⁴C were ±0.2 TU and ±0.4 pMC respectively.

The cation, anion and stable isotope measurements were performed at the State Key Laboratory of Biogeology and Environmental Geology, China University of Geosciences in Wuhan. Cations were analysed using an inductively coupled
180 plasma atomic emission spectrometry (ICP-AES) (IRIS Intrepid II XSP, Thermo Elemental). Anions were analysed on filtered unacidified samples using ion chromatography (IC) (Metrohm 761 Compact IC). Analytical errors were inferred from the mass balance between cations and anions (with HCO₃), and are within ±6 %. Stable isotopic values (δ²H and δ¹⁸O) analyses were measured using a Finnigan MAT-253 mass spectrometer (Thermo Fisher, USA, manufactured in Bremen, Germany), with the TC/EA method. The δ²H and δ¹⁸O values (Table 1) were presented in δ notation in ‰ with respect to the
185 Vienna Standard Mean Ocean Water (VSMOW), with an analytical precision of 0.5 ‰ vs. VSMOW for δ²H and of 0.1 ‰ for δ¹⁸O.

3.3 Groundwater dating

3.3.1 CFCs indicating modern water recharge

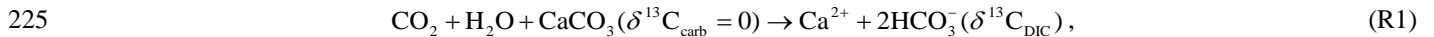
Knowledge of the history of the local atmospheric mixing ratios of CFCs in precipitation is first required for indicating
190 modern water recharge. The difference between the local and global background atmospheric mixing ratios of CFCs in the Northern Hemisphere – *CFC excess* – varies substantially based on the industrial development of the area. Elevated CFC

concentrations (10–15 % higher than those of the Northern Hemisphere as a whole) have been reported in the air of urban environments such as Las Vegas, Tucson, Vienna, and Beijing (Barletta et al., 2006; Carlson et al., 2011; Han et al., 2007; Qin et al., 2007). ~~Whereas~~ the atmospheric mixing ratios of CFCs in Lanzhou and Yinchuan (Northwest China) ~~they~~ were approximately 10 % lower than those of the Northern Hemisphere (Barletta et al., 2006). Manas River Basin is located in Northwest China (Fig. 1a), has a very low population density, and is far from industrial cities. To evaluate CFC ages, the time series trend of Northern Hemisphere atmospheric mixing ratio (Fig. 3; 1940–2014, <http://water.usgs.gov/lab/software/air/cure/>) was adopted in this study.

Measured CFC concentrations (in pmol L⁻¹) can be interpreted in terms of partial pressures of CFCs (in pptv) in solubility equilibrium with the water sample based on Henry's law. ~~Concrete~~ The computational process was conducted following Plummer et al. (2006a). In arid Northwest China, estimating the local shallow groundwater temperature as recharge temperature is more suitable than the annual mean surface air temperature (Qin et al., 2011) because the local low precipitation usually cannot reach the groundwater. Studies ~~On~~ on the MRB (Ji, 2016; Wu, 2007) have also indicated much less vertical recharge water from the local precipitation compared with abundant groundwater lateral flow recharge and river leakage from the mountain to the piedmont areas. In this study, the measured groundwater temperature, which varied from 11.5 to 15.7 °C between wells (Table 1), was used as the recharge temperature to estimate the groundwater input CFC concentrations. Surface elevations of the recharge area vary from 316 to 755 m. The modern water recharge was then determined by comparing the calculated partial pressures of CFCs in solubility equilibrium with the water samples with historical CFC concentrations in the air (Fig. 3).

3.3.2 The apparent ¹⁴C ages

Carbon-14 (¹⁴C, half-life: 5730 yrs) activity in groundwater is often used to estimate groundwater age over time periods of approximately 200 ~~and to~~ 30 000 yrs, and to determine the recharge from mixing water in various climate conditions (Cook, et al., 2017; Custodio et al., 2018; Huang et al., 2017). Since groundwater age cannot be measured directly, and the age distribution in the sample is unknown, one can derive an apparent age using a mathematical formula for the groundwater ¹⁴C sample (Suckow, 2014). "Apparent" here describe the fact that the age is not corresponding to the time difference between recharge and sampling during which piston flow is assumed for a water parcel (Cartwright et al., 2017; Suckow, 2014). Calculation of groundwater apparent ¹⁴C ~~groundwater~~ age may be complicated if dissolved inorganic carbon is derived from a mixture of sources, or if ¹⁴C originating from the atmosphere or soil zone is significantly diluted by the dissolution of ¹⁴C-free carbonate minerals in the aquifer matrix and biochemical reactions along the groundwater flow paths (Clark and Fritz, 1997). Although only minor carbonate dissolution is likely, determination of groundwater residence times requires ¹⁴C correction (Atkinson et al., 2014). When the dissolution of carbonate during recharge or along the groundwater flow path may dilute the initial soil CO₂, δ¹³C can be used to trace the process (Clark and Fritz, 1997). An equation for the reaction between CO₂-containing water with a carbonate mineral is commonly written as follows (modified after Pearson and Hanshaw, 1970):



where $\delta^{13}\text{C}_{\text{carb}}$ is the dissolved carbonate $\delta^{13}\text{C}$ value (approximately 0; Clark and Fritz, 1997), and $\delta^{13}\text{C}_{\text{DIC}}$ is the measured $\delta^{13}\text{C}$ value in groundwater.

Depending on knowing the measured ^{14}C activity after adjustment for the geochemical and physical dilution processes in the aquifer (without radioactive decay), the groundwater apparent ^{14}C ages (t) can be calculated from the following decay equation:

230

$$t = -\frac{1}{\lambda_{^{14}\text{C}}} \times \ln \frac{a^{14}\text{C}}{a_0^{14}\text{C}}, \quad (1)$$

where $\lambda_{^{14}\text{C}}$ is the ^{14}C decay constant ($\lambda_{^{14}\text{C}} = \ln 2/5730$), and $a^{14}\text{C}$ is the measured ^{14}C activity of the DIC in groundwater.

~~As mentioned above, the estimated ages are really apparent ages due to the mixture of waters with wide range of ages (Custodio et al., 2018; Suckow, 2014).~~

235 Previous studies in the arid ~~northwest~~Northwest China (Edmunds et al., 2006; Huang et al., 2017) have concluded that a volumetric value of 20 % “dead” carbon derived from the aquifer matrix was recognized, which is consistent with the value (10–25 %) obtained by Vogel (1970). Therefore, the initial ^{14}C activity ($a_0^{14}\text{C}$) of 80 pMC is used to correct groundwater ^{14}C ages (results are shown in Table 1), ~~despite-although~~ this simple correction makes no attempt to correct the age of individual samples that may have experienced different water–rock interaction histories.

240 3.3.3 Groundwater mean residence time estimation

Groundwater mixing may occur both within the aquifer and in the long–screened wells (Cook et al., 2017; Custodio et al., 2018; Visser et al., 2013). ~~A wide range of the groundwater residence times (ages) has been reported in an arid unconfined aquifer because recharge occurs under various climate conditions (Custodio et al., 2018). Furthermore, the groundwater residence time with wide variabilities that governed by the distribution of flow paths of varying length cannot be measured directly (de Dreuz and Ginn, 2016; Suckow, 2014). A lumped parameter model may be an alternative approach to describe the distribution of residence times, which at the same time describes a mean residence time for the mixtures of different residence times. The groundwater residence times (ages) often display a wide range because recharge occurs under various climate conditions (Custodio et al., 2018).~~ With the aid of gaseous tracers (e.g. ^3H , CFCs, SF_6 and ^{85}Kr) one can describe the ~~mixing~~ distribution of tracer concentrations using a mixing model (Stewart et al., 2017; Zuber et al., 2005) to obtain the groundwater MRTs. ~~LPMs is an alternative approach to interpret MRTs for water flow through the subsurface systems to the output.~~ For the steady–state subsurface hydrologic system, ^3H and CFCs tracers entering groundwater with precipitation are injected proportionally to the volumetric flow rates by natural processes. ~~‡~~ The output concentration in water at the time of sampling relating to the input ^3H and CFCs can be described by the following convolution integrals (Małoszewski and Zuber, 1982):

245

250

255

$$C_{\text{out}}(t) = \int_0^{\infty} C_{\text{in}}(t-\tau) g(\tau) e^{-\lambda_{3\text{H}}\tau} d\tau \quad \text{for } ^3\text{H tracer} \quad (2a)$$

$$C_{\text{out}}(t) = \int_0^{\infty} C_{\text{in}}(t-\tau) g(\tau) d\tau \quad \text{for CFCs tracer,} \quad (2b)$$

where C_{out} is the tracer output concentration, C_{in} is the tracer input concentration, τ is the residence time, $t-\tau$ is the time when water entered the catchment, $\lambda_{3\text{H}}$ is the ^3H decay constant ($\lambda_{3\text{H}} = \ln 2/12.32$), and $g(\tau)$ is the system response function that describes the residence time distributions (RTDs) in the subsurface hydrologic system.

260

265

270

In this study, the CFC concentrations from the time series trend of the Northern Hemisphere atmospheric mixing ratio (Fig. 3) and ^3H concentrations-activities in precipitation in Urumqi (Fig. 4) are treated as proxies for CFC and ^3H recharge concentrations (C_{in}), respectively. The historical precipitation ^3H activity in the Urumqi station (Fig. 4) is-was reconstructed with the data available from the International Atomic Energy Agency (IAEA) using a logarithmic interpolation method. The precipitation ^3H activity between 1969 and 1983 at Hong Kong and Irkutsk with different latitudes are-was used (data is available at <<https://www.iaea.org/>>). The time series of ^3H activity (Fig. 4) was-used as the input data are-was based on the following considerations. First, the MRB is located in the Northern Hemisphere, where the bomb-pulse ^3H activity is several orders of magnitude higher than in the Southern Hemisphere (Clark and Fritz, 1997; Tadros et al., 2014) and was superimposed with the China atmospheric nuclear tests from 1964 to 1974 in the arid regions-of Northwest China;-t. Thus, the remnant ^3H activity remains affected by the tail-end of the bomb pulse. Second, the study area is more than 3500 km away from the western Pacific, where-hence the atmospheric ^3H activity is much higher than that at coastal sites due to the continental effect (Tadros et al., 2014). Furthermore, although the atmospheric ^3H activity varies between seasons (Cartwright and Morgenstern, 2016; Morgenstern et al., 2010; Tadros et al., 2014), the-mean annual values (Fig. 4) were considered in this study.

275

280

Several RTDs-residence time distributions have been described (Małozzewski and Zuber, 1982; Jurgens et al., 2012) and have been widely used in studies of variable timescales and catchment areas (Cartwright and Morgenstern, 2015, 2016; Cartwright et al., 2018; Hrachowitz et al., 2009; Morgenstern et al., 2010, 2015; McGuire et al., 2005). The selection of each model depends on the hydrogeological situations in the hydrologic system to which it is applicable. The exponential-piston flow model (EPM) describes an aquifer that contains a segment of the exponential flow followed by a segment of piston flow. The piston flow model assumes minimal water mixing from different flow lines and little or no recharge in the confined aquifer; the exponential flow model assumes a full mixing of water in the unconfined aquifer and the receipt of areally distributed recharge (Jurgens et al., 2012; Małozzewski and Zuber, 1982). The weighting function of this model is given by

$$g(\tau) = 0 \quad \text{for } \tau < \tau_m(1-1/\eta) \quad (3a)$$

$$g(\tau) = \frac{\eta}{\tau_m} e^{(-\eta\tau/\tau_m + \eta - 1)} \quad \text{for } \tau \geq \tau_m(1-1/\eta) \quad (3b)$$

285 The dispersion model (DM) mainly measures the relative importance of dispersion to advection, and is applicable for confined or partially confined aquifers (Małoszewski, 2000). Its RTD-residence time distribution is given by

$$g(\tau) = \frac{1}{\tau \sqrt{4\pi D_p \tau / \tau_m}} e^{-\left(\frac{(1-\tau/\tau_m)^2}{4\pi D_p \tau / \tau_m}\right)} \quad (4)$$

The weighting function of the exponential mixing model (EMM) is

$$g(\tau) = \frac{1}{\tau_m} e^{(-\tau/\tau_m)}, \quad (5)$$

290 where τ_m is the mean residence time, η is the ratio defined as $\eta = (l_p + l_E)/l_E = l_p/l_E + 1$, where l_E (or l_p) is the length of area at the water table (~~or not~~) receiving (or not receiving) recharge, D_p is the dispersion parameter, which is the reciprocal of the Peclet number (Pe) and defined as $D_p = D/(vx)$, where D is the dispersion coefficient ($m^2 \text{ day}^{-1}$), v is velocity ($m \text{ day}^{-1}$), and x is distance (m).

295 Each RTD-residence time distribution has one or two parameters, MRTs (τ_m) ~~is-are~~ determined by convoluting the input (the time series of ^3H and CFCs input in rainfall) to each model to match the output (the measured ^3H and CFC concentrations in groundwater). ~~and~~ The other parameters (η and D_p) are determined depending on the hydrogeological conditions. To interpret the ages of the MRB data set, EPM ($\eta=1.5$ and 2.2), DM ($D_p=0.03$ and 0.1), and EMM models were used, after which MRTs ~~with different RTDs~~ were cross-referenced/compared.

4 Results and discussion

4.1 Stable isotope and major ion hydrochemistry

300 The $\delta^2\text{H}$ ~~and $\delta^{18}\text{O}$~~ values in the study area vary from -75.88 to -53.40 ‰ ~~and -11.62 to -6.76 ‰~~ for the surface water, and ~~from~~ -82.45 to -62.16 ‰ for the groundwater. Meanwhile, the $\delta^{18}\text{O}$ values vary from -11.62 to -6.76 ‰ for the surface water, and -12.19 to -9.01 ‰ for the groundwater. Figure 5a shows the $\delta^2\text{H}$ and $\delta^{18}\text{O}$ values of surface water and groundwater in relation to the precipitation isotopes of the closest GNIP station (Urumqi station in Fig. 1a). Both the linear slope (7.3) and intercept (3.1) of the Local Meteoric Water Line (LMWL) are lower than that of the Global Meteoric Water Line (GMWL, 8 and 10, respectively; Craig 1961). Surface water (ditch, river and reservoir water) ~~are-is~~ more enriched in heavy isotopes and ~~defined-defines~~ an evaporation line with a slope of 4.5 (Fig. 5b), which is much higher than that solely calculated from the upstream river water and reservoir water (slope=3.2 from Ma et al., 2018).

310 Groundwater deuterium excess values (d -excess = $\delta^2\text{H} - 8\delta^{18}\text{O}$, Fig. 5b) defined by Dansgaard (1964) lie close to the annual mean LMWL ($d_{\text{LMWL}}=13$ ‰), which also suggest little isotope fractionation by evaporation as d -excess value decreases when water evaporates (Han et al. 2011; Ma et al., 2015). The d -excess values of surface water decrease from 17.12 ‰ in the upstream area to 0.68 ‰ in the downstream area, indicating strong evaporation effect, which is also

demonstrated by the low slope (evaporation slope=4.5) of the surface waters. A recent study (Benettin et al., 2018) indicated that the evaporation line obtained from various sources of water is often not the true evaporation line. All samples of surface water in the present study were collected in the summer of 2015 and were recharged from the mountain areas in the same season. Although they were collected from different areas (ditch water, reservoir water, and Manas River water), the linear trend obtained may have implications for surface water evaporation.

The hydrochemistry compositions of surface water and groundwater in the MRB reflect the evolution from the fresh $\text{HCO}_3\text{-SO}_4\text{-Ca}$ water type to the $\text{HCO}_3\text{-SO}_4\text{-Na-Ca}$ type and further to the $\text{HCO}_3\text{-SO}_4\text{-Na}$ type, and finally to the brine $\text{Cl-SO}_4\text{-Na}$ water type along the groundwater flow paths (Fig. 6). Groundwater in the unconfined aquifers (e.g., intermountain depression and piedmont plain aquifers in Fig. 1c) is dominated by Ca^{2+} and HCO_3^- with a relatively low concentration of Na^+ (Fig. 6). Groundwater in the confined aquifers is characterised by a wide range of ion concentrations, with progressively increasing Na^+ and Cl^- ion concentrations, whereas Ca^{2+} and Mg^{2+} ion concentrations decrease progressively as the salinity spectrum moves towards the more concentrated end of the salinity spectrum (Fig. 6). The concentration of SO_4^{2-} ion gradually increases in the unconfined aquifers and becomes less dominant in the confined aquifers along the groundwater flow paths (Fig. 6).

4.2 Modern and paleo-meteoric recharge features

4.2.1 Stable isotope indications

Stable isotopes ($\delta^2\text{H}$ and $\delta^{18}\text{O}$), the components of the water molecule that record the atmospheric conditions at the time of recharge (Batlle-Aguilar et al., 2017; Chen et al., 2003), provide valuable information on groundwater recharge processes. Generally, there are two possible meteoric recharge sources including precipitation in the modern climate and in the paleoclimate. Groundwater whose isotopic values are more depleted than the modern precipitation usually would be ascribed to one or both of two recharge sources including snowmelt/precipitation at higher elevation and precipitation fallen during cooler climate. Figure 5 shows that the markers of groundwater isotopes generally do not define evaporation trend, implying that little evaporation and isotope exchange between groundwater and the rock matrix have occurred (Ma et al., 2018; Négrel et al., 2016). Transpiration over evaporation is likely to be dominant in the soil when infiltration as soil water uptake by root is not significantly isotope fractionated (Dawson and Ehleringer 1991).

Three groundwater clusters can be identified in the $\delta^2\text{H}\text{-}\delta^{18}\text{O}$ plot (Fig. 5b), suggesting different recharge sources among the upstream, midstream, and downstream areas. The first group of UG with the average $\delta^2\text{H}$ and $\delta^{18}\text{O}$ values of -68.24 and -10.08 ‰, respectively, Figure 5a shows that was from UG and is located much closer to the summer rainfall (Fig. 5a), which reflecting reflects more enriched summer rainfall inputs in the upstream area of the Manas River. Negligible evaporation trends were are observed in UG, although the recharge was mostly from in the summer due to the fast river leakage in the intermountain depression through highly permeable pebbles and gravel deposits (Fig. 1c). Furthermore, the detectable CFC concentrations and high ^3H activity (Table 1) also indicate a modern precipitation recharge. An overlap

345 between surface water and UG indicates the same recharge sources, because some alignment of river water and groundwater isotopic values ~~suggest-is~~ a qualitative indication of recharge under climate conditions similar to contemporary conditions (Huang et al., 2017).

350 The second group ~~with-has the~~ average $\delta^2\text{H}$ and $\delta^{18}\text{O}$ values of -73.10 and -11.0 ‰, respectively, which overlap overlapped with the annual amount-weighted mean rainfall isotopic value from MG. Such isotopic values are comparable to the modern annual amount-weighted mean rainfall $\delta^2\text{H}$ and $\delta^{18}\text{O}$ values (-74.7 and -11.0 ‰, respectively; Fig. 5a), it probably reflects sing annual modern precipitation recharge. The mixing of different time-scale recharges of variable isotopic values at different aquifers and sites along the groundwater flow paths is ~~Another-another~~ explanation for the relatively highly scattered MG isotopic values in the $\delta^2\text{H}$ - $\delta^{18}\text{O}$ plot (Fig. 5b) ~~is mixing with different time-scale recharges of variable isotopic values at different aquifers and sites along the groundwater flow paths~~. Groundwater isotopes in the piedmont plain are relatively rich in heavy isotopes (Fig. 5b), which overlap with the river water, indicating-and indicate fast river leakage recharge ~~in-within~~ a short time (Ma et al., 2018). Groundwater ~~isotopes-isotopic values~~ in the oasis plain diverge from those in the piedmont plain (Fig. 5b) and do not align with surface water, indicating recharge with longer flow paths rather than fast river leakage recharge.

360 The third group, which is the most depleted in heavy isotopes (-82.36 and -12.03 ‰), ~~was-is~~ from DG and ~~was-is~~ located much closer to the winter rainfall in the $\delta^2\text{H}$ - $\delta^{18}\text{O}$ plot (Fig. 5b). Studies (Ji, 2016; Ma et al., 2018) have shown that vertical recharge from the winter rainfall in the downstream area is unlikely. As ~~the-altitude-effects-of~~ precipitation recharge from high altitude (Clark and Fritz, 1997) and paleo-meteoric recharge during the cooler climate (Chen et al., 2003) could collectively account for the ~~isotopically depleted-depletion of isotopes in~~ groundwater, it is usually not easy to distinguish the precipitation recharge sources at a higher elevation from paleo-meteoric recharge. However, precipitation in the North Tianshan Mountain (Fig. 1a) have ~~the~~ positive isotope altitude gradient ~~of isotopes in precipitation due to the moisture recycling~~ (Kong and Pang, 2016) ~~over North Tianshan Mountain (Fig. 1a) was attributed to moisture recycling, and thus~~ sub-cloud evaporation effects ~~would-will~~ yield more enriched isotopes from higher-altitude precipitation recharge. The isotopically enriched UG (Fig. 5b) in the intermountain depression with higher altitude (Fig. 1c) ~~was-is~~ recharged from the high mountains. This also ~~demonstrated-demonstrates~~ that DG is unlikely to be from the high mountain recharge. Accordingly, its depleted isotopic values (Fig. 5b) ~~were-are~~ attributed to the paleo-meteoric recharge in a cooler climate. In 370 the last glacial period, temperatures in Xinjiang region (Li et al., 2015) and North China Plain (Chen et al., 2003) were cooler by approximately 10 °C and $6-9$ °C, respectively, compared with the present-day. Groundwater had a depleted $\delta^{18}\text{O}$ value of -12.0 ‰ from the paleo-meteoric recharge in the arid ~~regions-of~~ Northwest China, such as in the Minqin basin (Edmunds et al., 2006), as well as in the East (Li et al., 2015) and West (Huang et al., 2017) Junggar Basin (Fig. 1a).

4.2.2 CFCs indications

375 Table 1 shows that groundwater with well depths of 13–150 m contained detectable CFC concentrations ($0.17-3.77$ pmol L⁻¹ for CFC-11, $0.19-2.18$ pmol L⁻¹ for CFC-12, and $0.02-0.38$ pmol L⁻¹ for CFC-113) in both the upstream and midstream

380 areas, indicating at least a small fraction of young groundwater components (post-1940). The highest concentration ~~was-is~~ observed in the UG (G3), south of the fault. The median and the lowest ~~concentrations were-are~~ observed in the west and east banks, respectively, of the East Main Canal in the MG, north of the fault. In the midstream area (Fig. 2), CFC concentrations generally ~~decrease~~d with well depth south of the reservoirs (G25, G8, and G9), and ~~increase~~d with well depth north of the reservoirs (G15 and G16), which ~~might-may~~ indicate different groundwater flow paths (e.g., downward or upward flow directions).

385 The groundwater aerobic environment (Table 1, DO values ~~vary~~ from 0.7 to 9.8 mg L⁻¹) makes CFC degradation under anoxic conditions unlikely. Nevertheless, CFC-11 has shown a greater propensity for degradation and contamination than CFC-12 (Plummer et al., 2006b). ~~Therefore,~~ we use CFC-12 to interpret the modern groundwater recharge in the following discussions. The estimated CFC partial pressure and possible recharge year are shown in Table 2 and Fig. 3. The UG (G3) CFC-113 and CFC-12 both indicate the 1990 precipitation recharge (Table 2), ~~probably-most likely as~~ a piston flow recharge in the upstream area. The MG CFC-11-based modern precipitation recharge ~~was-is~~ in agreement with that based on CFC-12 concentrations within 2–8 yrs, whereas the CFC-113-based recharge ~~was-is~~ as much as 4–11 yrs later than that ~~of~~ 390 the other two, signifying recharge of a mixture of young and old groundwater components in the midstream area. The most recent groundwater recharge ~~was-is~~ in the upstream area (G3 with 1990 rainfall recharge), which ~~was-is~~ most likely because the flow paths from recharge sources here ~~were-are~~ shorter than those of the piedmont groundwater samples in the midstream area.

395 G5 and G7 ~~were-are~~ located in the east bank of the East Main Canal in the midstream area and ~~were-are~~ closer than G15 and G16 north of the reservoir, showing that the modern recharge ~~was-is~~ much earlier than that of G15 and G16 (Table 2). This ~~could-can~~ be explained by the lower groundwater velocities in the east bank of the East Main Canal, where the hydraulic gradient (Fig. 2) ~~was-is~~ much smaller than that in the west. Furthermore, groundwater recharge ~~south of the reservoir (G25, G8 and G9)~~ becoame earlier with increasing well depth from 48 to 100 m ~~south of the reservoir (G25, G8 and G9)~~, whereas that north of the reservoir becoame later with increasing well depth from 23 to 56 m (G15 and G16; Table 400 2, Fig. 2). The different trends for the relationship between groundwater recharge year and well depth ~~might-may~~ be due to the different flow paths between the two sites ~~(e.g., reservoir south and north)~~.

405 Comparing CFC concentrations helps to ~~indicate-identify~~ samples containing young (post-1940) and old (CFC-free) water (Han et al., 2007; Han et al., 2012; Koh et al., 2012) or exhibiting contamination or degradation (Plummer et al., 2006b). The cross-plot of the concentrations for CFC-113 and CFC-12 (Fig. 7a) demonstrates that all of the groundwater can be characterised as binary mixtures between young and older components, though there is still room for some ambiguity around the crossover in the late 1980s (Darling et al., 2012). As shown in Fig. 7a, all of the MG samples ~~are-were~~ located in the shaded region, representing no post-1989 water recharge. The UG (G3) sample is clearly relatively modern and seems to have been recharged in 1990 through piston flow or mixed with old water and post-1995 water. Using the method described by Plummer et al. (2006b) with the binary mixing model, the fractions of young water ~~were-are~~ found to vary from 12 to 91 % 410 (Table 2) for the MG samples with the relatively low young fractions of 12 and 18 % in the MG samples ~~(G5 and G7)~~ from

415 ~~the~~ east bank of the East Main Canal (~~G5 and G7~~). These two well water tables ~~were-are~~ deeper than 40 m, ~~probably~~
~~indicatingsuggesting~~ a relatively slow and deep circulated groundwater flow. This hypothesis is also suggested by the lower
DO (3.7–4.6 mg L⁻¹; Table 1) and nitrate concentrations (8.6–9.5 mg L⁻¹ from Ma et al., 2018), and ~~the~~ considerably smaller
hydraulic gradient (Fig. 2). Furthermore, a fraction of young water as high as 100 % ~~was-is~~ obtained ~~for-from the~~ G3 sample
with the recharge water from 1990, and ~~an~~ 87 % fraction ~~was-is~~ obtained ~~by~~ from the binary mixture of post-1989 water and
old water (Table 2). The relatively modern recharge for the G3 sample ~~was-is~~ likewise ~~explained-supported~~ by its high DO
(9.8 mg L⁻¹; Table 1) and relatively low nitrate concentration (7.9 mg L⁻¹ from Ma et al., 2018), which represent~~ed~~ the
contribution of high-altitude recharge rather than ~~the~~ old water.

420 CFC contamination and sorption in the unsaturated zone during recharge considerably influence~~d~~ the interpretation of
groundwater recharge. Points off the curves in the cross-plot of CFC concentrations may indicate contamination ~~with CFCs~~
from the urban air ~~with CFCs~~ during sampling (Carlson et al., 2011; Cook et al., 2006; Mahlknecht et al., 2017) or the
degradation or sorption of CFC-11 or CFC-113 (Plummer et al., 2006b). Figure 7 demonstrates that ~~CFC contamination~~
~~from~~ the urban air ~~with CFC contaminations~~, which generally ~~increased-increases~~ CFC concentrations above the global
background atmospheric CFC concentrations for the Northern Hemisphere, are unlikely. Elevated CFC concentrations have
425 been reported in the air of urban environments such as Las Vegas, Tucson, Vienna and Beijing (Barletta et al., 2006; Carlson
et al., 2011; Han et al., 2007; Qin et al., 2007), ~~but not rather than~~ in the arid ~~regions-of~~ Northwest China (Barletta et al.,
2006). Hence, the anomalous ratios of CFC-11/CFC-12 (Fig. 7b) off the model lines ~~might-may~~ be attributed to sorption in
the unsaturated zone during recharge ~~rather thanbut not~~ the degradation of CFC-11 (Cook et al., 2006; Plummer et al., 2006b)
under anoxic conditions (Table 1, DO values vary from 0.7 to 9.8 mg L⁻¹). Nevertheless, the small deviations (Fig. 7b)
430 indicate a low sorption rate. A higher CFC sorption rate occurs with high clay fraction and high organic matter in soils
(Russell and Thompson, 1983), and vice versa (Carlson et al., 2011). Therefore, the hypothesis of a low sorption rate due to
the low clay fraction and low organic matter content in the intermountain depression and the piedmont plain (Fig. 1c) ~~seems~~
~~is~~ reasonable.

435 The time lag for CFC transport through the thick unsaturated zone (Cook and Solomon, 1995), as well as degradation,
especially for CFC-11 being common in anaerobic groundwater (Horneman et al., 2008; Plummer et al., 2006b), are both
important considerations when interpreting groundwater recharge using CFC concentrations. The time lag for CFC
diffusions through the deep unsaturated zone in simple porous aquifers, a function of the tracer solubility in water, tracer
diffusion coefficients, and soil water content (Cook and Solomon, 1995), have been widely proved (Darling et al., 2012; Qin
et al., 2011). The small differences in CFC-11 and CFC-12 recharge years (Table 2) demonstrate that the time lag should be
440 short in the ~~faulted-fault-influenced~~ hydraulic drop alluvium aquifers with the deep unsaturated zone (Fig. 1c). Studies on
the MRB (Ma et al., 2018; Wang, 2007; Zhou, 1992) have shown that groundwater ~~is~~ mainly recharged by ~~the river~~ fast ~~river~~
leakage in the upstream area and piedmont plain, where the soil texture consists of pebbles and sandy gravel (Fig. 1c); ~~†~~ This
suggests that the unsaturated zone air CFC closely follows that of the atmosphere, so the recharge time lag through the
unsaturated zone is not considered.

445 4.2.3 ^3H and ^{14}C indications

Groundwater recharge was ~~be~~-determined using ^{14}C activity in groundwater for time intervals from centuries to ~~millenniums~~
~~millennia~~ (Custodio et al., 2018), and ^3H has been used for modern precipitation recharge, especially during the nuclear
bomb periods (Cook et al., 2017; Huang et al., 2017). Groundwater ^3H activity ~~varied-vary~~ from ~~1.1 to 60 to 1.1~~-TU (Fig. 4
and Table 1), with the highest value in UG (G4), followed by MG (mean 12.4 TU) and DG (mean 4.5 TU). All of the ^3H
450 values in UG (G1, G2, and G4) and G23 (belonging to MG) ~~were-are~~ higher than 34.3 TU, which indicat~~ed~~ ~~input of~~ some
fractions of the 1960s precipitation recharge. Groundwater with ^3H activity lower than 5.6 TU contain~~ed~~ some pre-1950s
recharge.

Both ^3H and ^{14}C activities show~~ed~~ large variations with the distance to the mountainous region along groundwater flow
paths in the midstream area (Fig. 8), suggesting recharge over a mixture of short to long timescales. Two different trends for
455 the distribution of ^3H activity with distance to the mountainous region (Fig. 8) from the upstream to midstream areas ~~were~~
~~are~~ observed. First, ~~in the upstream area an~~ increase in ^3H activity ~~with distance in groundwater in the upstream area is seen~~
from 41.1 (G1 and G2) to 60 TU (G4), ~~with distance indicated~~~~indicating~~ a larger fraction of 1960s precipitation for G4 than
for G1 and G2; indeed, as seen in Fig. 2, near G4 samples exhibited the highest hydraulic gradient values. Second, ^3H
activity in groundwater in the midstream area show~~ed~~ an obvious reduction trend along the Manas River from 37.5 (G23) to
460 1.1 TU (G14), indicating that more fractions of pre-bomb precipitation recharge may have occurred along the groundwater
flow direction ~~in the~~-north of the fault. Furthermore, ^{14}C activity in the MG showed small increases with distance (Fig. 8)
from 43.4 to 54.6 pMC, with the exception of sample G12 at approximately 54 km (86.9 pMC with a $^{14}\text{C}_{\text{corr}}$ age of -684 yrs;
modern recharge; Table 1), whereas that in the DG decrease~~ed~~ to 23.5 pMC. The presence of detectable ^3H (2.9–6.91 TU) in
DG with low ^{14}C values (23.5–34.3 pMC) indicat~~ed~~ that some mixing with post-bomb precipitation recharge may have
465 occurred.

Combined use of CFCs and ^3H may help ~~to~~ resolve even more complicated recharge features due to the large difference of
the temporal pattern in the input functions between CFCs and ^3H . Compared with plots ~~comparing-of~~ tracer ratios, tracer-
tracer concentration plots have some advantages because they reflect more directly the measured quantities and potential
mixtures (Plummer et al., 2006b), such as mixing with irrigation water (Han et al., 2012, 2015; Koh et al., 2012) or young
470 water mixtures in different decades (Han et al., 2007; Qin et al., 2011). The plot of ^3H vs. CFC-12 (Fig. 9; CFC-11 and
CFC-113 can substitute for CFC-12) shows that some samples (G9, G15 and G20) are slightly above the piston flow line,
whereas in Fig. 7a they are away from the piston flow line but on the binary mixing lines. G15 and G20 ~~had-have~~ the
shallowest well depths of 23 and 13 m, respectively. The G9 sample was collected from the piedmont plain near Manas
River (Fig. 2), which features pebbles and sandy gravel deposits. This situation may be explained by (i) binary mixing
475 between post-1989 water and older water recharged between 1950 and 1970 that did not contain CFC-free water (pre-1940),
or (ii) mixing of two end-members with one end-member containing various mixtures of young (but pre-1989) and old
water and the other ~~end-member~~-having post-1989 water. The second explanation requires samples to contain at least some

post-bomb fractions from the 1960s (revealed by ^3H concentrations/activities; Fig. 9) and both post-1989 and pre-1940 water, which is not consistent with CFC data (Fig. 7a). If the first explanation is true, the binary mixing hypothesis and the young water (post-1940) fractions in Table 2 for these three samples should be adjusted accordingly.

Because atmospheric ^3H concentrations/activities have been elevated for a long time, old water components can be identified by ^3H concentrations/activities that are anomalously low compared with those of CFCs (Plummer et al., 2006b). The G5 sample contained very low CFC-113 with a ^3H concentration of 3.8 TU (Table 1), indicating that this sample was likely a mixed mixture of the older water (pre-1940) and 1960-1970 water. The low ^3H concentration can be attributed to the dilution by a high fraction of old water, and thus the " ^3H bomb-peak" cannot be recognised. The G16 sample, outside of the shaded region (Fig. 9), has low ^3H but a substantial CFC concentration. This situation may be explained by (i) exposure to the atmosphere before sampling during large water table fluctuations due to groundwater pumping or the addition of excess air to water through the fractured system, or (ii) river water or reservoir water with high CFC concentration but minimal ^3H recharge. Furthermore, the relatively high fractions of young water (89 %; Table 2) preclude the dilution effect by the old water. Irrigation re-infiltration can cause a shift of the CFC concentrations to higher values but does not alter the ^3H concentration (Han et al., 2015). However, the relatively low NO_3^- concentrations (4.51 mg L^{-1} ; data from Ma et al., 2018) of the G16 sample suggested that irrigation re-infiltration did not have a significant effect. Therefore, river or reservoir water with very low NO_3^- concentration ($2.7\text{--}7.3 \text{ mg L}^{-1}$; data from Ma et al., 2018) recharge is possible.

4.3 Groundwater mean residence time

4.3.1 ^3H and CFCs

Residence time distribution (RTD) functions (Eqs. (3) to (5)) are suited to for several specific hydrogeological situations (Małozzewski and Zuber, 1982); EPM is particularly useful for the interpretation of MRTs in aquifers that have regions of both exponential and piston flow (Cartwright et al., 2017). The unconfined aquifers adjacent to the rivers (Fig. 1 c) are likely to exhibit exponential flow, and the recharge through the unsaturated zone (Fig. 1c) will most likely resemble piston flow (Cartwright and Morgenstern, 2015; Cook and Böhlke, 2000). For the time series of ^3H and CFCs inputs, MRTs (Fig. 10) were initially calculated using EPM, with an EPM ratio of 1.5 obtained using Eqs. (2) and (3) (I_e in Eq. (3) is determined by adding the intermountain depression to the piedmont plain in Fig. 1c). River leakage and rainfall input were possible only from the piedmont plain (Ma et al., 2018), thus a smaller proportion of piston flow by in the EPM with could give an EPM ratio of 2.2 (I_e in Eq. (3) is only in would only be for the piedmont plain in Fig. 1c). The veracity of MRTs are tested by Eqs. (2), (4) and (5) using the DM ($D_p = 0.03$ or 0.1) with D_p of 0.03 and 0.1 and the EMM were also used to calculate the MRTs via Eqs. (2), (4) and (5). Plots of the output concentrations for ^3H (Fig. 10a) and CFCs (CFC-11 in Fig. 10b, CFC-12 in Fig. 10c and CFC-113 in Fig. 10d) vs. MRTs for different lumped parameter models show that the range of wide-MRTs ranges that increase with the increasing are wide and positively response to the increase of MRTs.

510 Figure 11 shows that presents different LPMs yield different MRTs for the same determined from the time series of ^3H and CFC concentrations inputs using different lumped parameter models. MRTs obtained from different lumped parameter models LPMs tend to become more discretized by model with increasing of the MRTs themselves. For the CFC rainfall inputs, On the other hand, MRTs estimated from the EPM with an EPM ratio of 1.5 (in Fig. 11a) varied vary from 19 to 101 yrs (median: 51 yrs) for the CFC-12 rainfall input, from 33 to 115 yrs (median: 62.3 yrs) for the CFC-11 rainfall input, and from 18 to 92 yrs (median: 50.2 yrs) for the CFC-113 rainfall input. Good linear relationships for MRTs between the different CFCs rainfall inputs were are obtained using the same EPM (EPM (1.5) in Fig. 11a and EPM (2.2) in Fig. 11b). MRTs increased when the EPM ratios decrease from 2.2 to 1.5 in Fig. 11b, with decreasing EPM ratios (from 2.2 to 1.5; Fig. 11b), implying that the longer groundwater flow paths were recharged from the intermountain depression are much longer. For the range of CFC-12 concentrations MRTs in the UG, and in the west and east banks of the East Main Canal of MG are estimated from the different lumped parameter models with different CFC-12 concentrations in Figs. 2 and 11b. The mean values of MRTs in the UG and the west bank of the East Main Canal of MG vary from 28.6 to 64.8 yrs, and in the east bank of the East Main Canal of MG vary from 129.2 to 173 yr. It is seen that the mean values of MRTs in the east bank of the East Main Canal of MG are larger differences than those in the UG and in the west bank of the East Main Canal of MG (see Figs. 2 and 11b, and Table 2). Similar MRTs were estimated from the different LPMs (Fig. 11b) with mean values varying from 28.6 to 64.8 yrs, whereas those in the east bank (Figs. 2 and 11b and Table 2) of MG show larger differences with mean values varying from 129.2 to 173 yrs. Overall, the youngest value was is observed in the G3 sample (on the south side of the fault), and the oldest was value is observed in the G5 sample on the east bank of the East Main Canal; in Fig. 2).

520 In contrast to the CFC rainfall inputs, MRTs estimated using the ^3H rainfall inputs by different LPMs (Fig. 11c) show larger uncertainties and wider ranges. It is seen from Fig. 11 that MRTs determined from the time series of ^3H inputs have larger uncertainties and wider ranges than those from CFCs. For EPM with an EPM ratio of 1.5, MRTs estimated from the time series ^3H inputs vary from 19 to 158 yrs with a median of 112.2 yrs (Fig. 11c), which are much longer than those calculated from the CFCs rainfall inputs by the same model (Fig. 11b). The differences could be due to reason is that the longer travel times through the thick unsaturated zone for ^3H are much longer than those for CFCs. ^3H moves principally in the liquid phase, whereas CFCs travel in the gas phase through the unsaturated zone (Cook and Solomon, 1995). The more rapid transport for of gas phase is more rapid than that of liquid phase in the unsaturated zone, which would be expected to give rise to longer residence times from ^3H than those determined from CFCs (Cook, et al., 2017). Furthermore, the ranges in of MRTs estimated from EPM with EPM ratios of 1.5 and 2.2, DM with D_p of 0.03 and 0.1, and EMM are 16–158 yrs, 72–285 yrs, and 30–360 yrs, respectively. Similar MRT trends were calculated from the CFC-12 input (Fig. 11b), in which the west and east banks of the East Main Canal of MG and DG were separated. The uncertainties will increase with when MRTs increasing MRTs among the different models, especially when for MRTs that are higher than 130 yrs (Fig. 11c), which mainly occurred exists in the DG and samples collected from the east bank of the East Main Canal of MG and DG.

540 Groundwater MRTs in the west bank of the East Main Canal shows an overall increasing trend with the distance to mountain in MG and DG (Fig. 11b, c). It has been proven that much longer as well as much deeper flow paths usually give

545 rise to much longer MRTs (Cartwright and Morgenstern, 2015, 2016; McGuire et al., 2005). On the other hand, groundwater
MRTs in the east bank of the East Main Canal are much longer than those in the west bank. As shown in Fig. 2, this
phenomenon can partly be ascribed to the relatively short distance to mountain and much smaller hydraulic gradient in the
west bank. Because the east bank groundwater had a relatively short distance to mountain and a much smaller hydraulic
gradient (Fig. 2), the MRTs were much longer than those in the west bank. That in the west bank shows an overall increasing
550 trend with the distance to mountain in MG and DG (Fig. 11b, c) as the longer and deeper flow paths usually give rise to the
longer MRTs (Cartwright and Morgenstern, 2015, 2016; McGuire et al., 2005). Previous studies pointed that groundwater
MRTs would vary on account of interplay of factors, like the uncertainties of the input concentrations and different models
(Cartwright and Morgenstern, 2015, 2016), and mixing and dispersion in the subsurface flow systems. Despite the influence
from the uncertainties of the input concentrations and different models (Cartwright and Morgenstern, 2015, 2016), MRTs
have been identified to vary on account of more complex interplay of factors like mixing and dispersion in the flow systems.
555 Moreover, the assumption of the homogeneous aquifer with a simple geometry which may result in significantly different
MRTs from results that calculated by lumped parameter models (LPMs) assuming a homogeneous aquifer with a simple
geometry to the actual results-MRTs (Cartwright et al., 2017; Kirchner, 2016; Stewart et al., 2017). Nevertheless, in this
study the homogeneous aquifers, being at steady-state, justifying the use of LPMs-lumped parameter models to calculate
MRTs in this study.

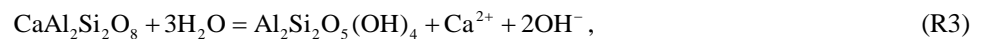
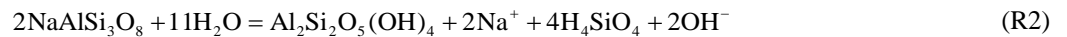
560 4.3.2 Hydrochemistry evolution

Strong correlations between hydrochemical components and groundwater age permit their use as proxies for, or
complementary to, age via previously established relationships in ~~close-similar~~ lithological conditions. For example, an
excellent correlation between silica (SiO_2) and MRTs ($R^2=0.997$) ~~was-has been~~ reported (Morgenstern et al., 2010), which
was much ~~higher-better~~ than in Fig. 12 and in other results (Morgenstern et al., 2015). SiO_2 (Fig. 12a), sulfate (SO_4^{2-}),
565 bicarbonate (HCO_3^-), and total dissolved solids (TDS) (Fig. 12b) all show good correlations with groundwater age,
indicating that mineral dissolutions through water-rock interactions dominate hydrochemical changes (Ma et al., 2018), and
major ion concentrations increase with groundwater age. However, MRTs ~~estimated-using~~ determined by the time series of
 ^3H ~~activity-inputs~~ showed poor correlations with the ions (data not shown). Moreover, the lithology type ~~that the~~
groundwater flows through within the aquifer, and the likely evolutionary path ways, play ~~an~~ important roles in the
570 hydrochemical compositions. The negative saturation indices with respect to gypsum ~~of all water~~ (Ma et al., 2018) indicated
that the high SO_4^{2-} concentrations (Fig. 12b) ~~were-are~~ due to the gypsum dissolution in the Tertiary stratum. ~~It is also of~~ Also
note that high SO_4^{2-} can be originated from ~~the~~ geothermal water (Morgenstern et al., 2015), in contrast to studies such as
Guo et al. (2014) and Guo et al. (2017), and can be biased due to anoxic SO_4^{2-} reduction. However, the groundwater ~~with-in~~
this study have relatively low temperatures and aerobic environment (Table 1), making the two cases above unlikely.

575 The combination of hydrochemistry concentrations and groundwater age data is also a powerful tool for investigating the
groundwater flow processes and flow through conditions (McGuire and McDonnell, 2006; Morgenstern et al., 2010, 2015),

and for identifying the natural groundwater evolution and the impact of anthropogenic contaminants (Morgenstern et al., 2015; Morgenstern and Daughney, 2012). The pH of the groundwater decreases from 10.1 to 8.6 over the age range from 19 to 101 yrs, with a log law fit of $\text{pH} = 0.72 \times \ln(\text{MRTs}) + 11.85$, $R^2 = 0.65$ (Fig. 12a). ~~On the contrary~~In contrast, a trend of increasing pH with increasing groundwater age has been reported in New Zealand (the dashed red line shown in Fig. 12a; Morgenstern et al., 2015), where ~~the~~ pH values were ~~overall~~ less than 7.2. These two discrepant trends can be explained by the relationship between ~~the~~ pH and HCO_3^- concentrations in water (inserted plot in Fig. 12a), ~~which is~~The pH increases with increasing HCO_3^- concentrations ~~only~~ when the pH is less than 8.34, otherwise it decreases with increasing HCO_3^- concentrations. Therefore, the trend of increasing HCO_3^- concentrations with increasing groundwater age (Fig. 12b) in this study ~~indicates~~supports the that decreasing trend for the pH (from 10.1 to 8.6) ~~is reasonable~~.

The soda waters with ~~the~~an overall pH higher than 8.1 (Table 1) are in disequilibrium with primary rock-forming minerals of the host rocks. The incongruent dissolutions of the albite and anorthite through hydrolysis reaction are:



where all ~~the~~ chemical components of ~~the~~ albite and anorthite release into the solution phase and produce OH^- with simultaneous precipitation of kaolinite. A trend of increasing pH with well depth (Table 1) suggests that groundwater with whose pH is lower than 9 ~~was is~~ likely recharged by CO_2 -containing water, because OH^- generally interacts with CO_2 and organic acids in the soil to form HCO_3^- (Wang et al., 2009). Similarly, the trend of decreasing pH with increasing MRTs (Fig. 12a) indicates that ~~water groundwater with much longer MRTs contains much~~containing higher CO_2 concentrations ~~has longer MRT~~, which seems to suggest ~~the~~an anthropogenic input. The nitrate (NO_3^-) concentrations ~~varied vary~~ from 4.5 to 20.2 mg L^{-1} with a median of 12.2 mg L^{-1} (data not shown), which exceeded the natural nitrate concentration in groundwater of 5–7 mg L^{-1} (Appelo and Postma, 2005). The development of the plough after the 1950s, N– NO_3 fertiliser (with low $^{87}\text{Sr}/^{86}\text{Sr}$ ratios; Ma et al., 2018), and the extensive groundwater withdrawal for irrigation (Ji, 2016) suggest that irrigation infiltration ~~could can~~ account for the high groundwater NO_3^- concentrations in the piedmont plain. ~~However~~On the other hand, little irrigation infiltration was observed in the downstream area with groundwater NO_3^- concentrations of less than 5 mg L^{-1} (Ma et al., 2018) due to the water-saving irrigation style, which ~~did does~~ not contribute to groundwater recharge in the arid ~~regions of~~ Northwest China.

5 Conclusions

In this study, we used environmental tracers and hydrochemistry to identify the modern and paleo-meteoric recharge sources, to constrain the different end-members mixing ratios, and to study the mixed groundwater MRTs in ~~faulted-fault-influenced~~ hydraulic drop alluvium aquifer systems. ~~The paleo-meteoric recharge in a cooler climate was distinguished from the lateral flow from the higher elevation precipitation in the~~The aquifer below the Manas River downstream area is recharged by the

610 ~~paleo-meteoric precipitation instead of the lateral flow from higher elevation region.~~ The relatively modern groundwater with young (post-1940) water fractions of 87–100 % ~~was-is~~ obtained on the south side of the fault, indicating only a small ~~extent of mixing ratio between old and young watersouth of the fault.~~ The NO₃⁻ concentration (7.86 mg L⁻¹) is higher than the natural level; this, together with the short MRTs (19 yrs) ~~on the along with the higher than natural NO₃⁻ concentration (7.86 mg L⁻¹)-south side of the fault (headwater area),~~ implies indicated the invasion of modern contaminants. This finding ~~warrants-requires~~ particular attention since the headwater is used as the domestic water supply for local communities. The young water fractions of 12 to 91 % are widespread on the north side of the fault, suggesting that mixing between water of
615 different ages may occur within the aquifer or pumping from the different depths of long-screened boreholes. ~~High mixing rate amplitudes varying from 12 to 91 % were widespread in north of the fault due to the varying depths of long-screened boreholes as well as within the aquifer itself.~~ Furthermore, the mixing diversity ~~was-is~~ highlighted by the substantial water table fluctuations during groundwater pumping, vertical recharge through the thick unsaturated zone, and ~~young-water mixtures in different decades~~different young water inputs in different decades. The strong correlations between the
620 groundwater MRTs and the hydrochemical concentrations enable a first-order proxy at different times to be used. In addition, this study ~~has-revealed~~reveals that MRTs estimated by CFCs ~~were-are~~ more appropriate to be used as age proxy than those ~~using-estimated by~~ ³H in the arid MRB-Manas River Basin with a thick unsaturated zone.

Author contributions. Xing Liang and Jing Li were responsible for the ³H and ¹⁴C analyses. Bin Ma undertook the sampling program and oversaw the analysis of the hydrochemistry and CFCs. Bin Ma and Menggui Jin prepared the manuscript.

625 *Competing interests.* The authors declare that they have no conflict of interest.

Acknowledgements. This research was financially supported by the National Natural Science Foundation of China (no. U1403282 and no. 41807204). The authors would like to thank Dr. Yunquan Wang for the valuable discussions and suggestions for this paper. We wish to thank Dr. Xumei Mao, Dr. Dajun Qin and Mr. Yalei Liu for sampling and laboratory works. We also wish to thank the editor and anonymous referees for their valuable suggestions and insightful comments.

630 **References**

Aggarwal, P. K.: Introduction, in: Isotope Methods for Dating Old Groundwater, Suckow, A., Aggarwal, P. K., and Araguas-Araguas, L. (Eds.), International Atomic Energy Agency, Vienna, Austria, 1–4, 2013.

Appelo, C. A. J. and Postma, D.: Geochemistry, groundwater and pollution, 2nd ed., Balkema, Dordrecht, Netherlands, 2005.

- Atkinson, A. P., Cartwright, I., Gilfedder, B. S., Cendón, D. I., Unland, N. P., and Hofmann, H.: Using ^{14}C and ^3H to understand groundwater flow and recharge in an aquifer window, *Hydrol. Earth Syst. Sci.*, 18, 4951–4964, doi:10.5194/hess-18-4951-2014, 2014.
- 635
- Barletta, B., Meinardi, S., Simpson, I. J., Rowland, F. S., Chan, C. Y., Wang, X., Zou, S., Chan, L. Y., and Blake, D. R.: Ambient halocarbon mixing ratios in 45 Chinese cities, *Atmos. Environ.*, 40, 7706–7719, doi:10.1016/j.atmosenv.2006.08.039, 2006.
- 640
- Battle–Aguilar, J., Banks, E. W., Batelaan, O., Kipfer, R., Brennwald, M. S., and Cook, P. G.: Groundwater residence time and aquifer recharge in multilayered, semi–confined and faulted aquifer systems using environmental tracers, *J. Hydrol.*, 546, 150–165, doi:10.1016/j.jhydrol.2016.12.036, 2017.
- Benettin, P., Volkmann, T. H. M., Freyberg, J., Frentress, J., Penna, D., Dawson, T. E., and Kirchner, J. W.: Effects of climatic seasonality on the isotopic composition of evaporating soil waters, *Hydrol. Earth Syst. Sci.*, 22, 2881–2890, doi:10.5194/hess-22-2881-2018, 2018.
- 645
- Beyer, M., Jackson, B., Daughney, C., Morgenstern, U., and Norton, K.: Use of hydrochemistry as a standalone and complementary groundwater age tracer, *J. Hydrol.*, 543, 127–144, doi:10.1016/j.jhydrol.2016.05.062, 2016.
- Carlson, M. A., Lohse, K. A., McIntosh J. C., and McLain J. E. T.: Impacts of urbanization on groundwater quality and recharge in a semi–arid alluvial basin, *J. Hydrol.*, 409, 196–211, doi:10.1016/j.jhydrol.2011.08.020, 2011.
- 650
- Cartwright, I., Cendón, D., Currell, M., and Meredith, K.: A review of radioactive isotopes and other residence time tracers in understanding groundwater recharge: Possibilities, challenges, and limitations, *J. Hydrol.*, 555, 797–811, doi:10.1016/j.jhydrol.2017.10.053, 2017.
- Cartwright, I., Irvine, D., Burton, C., and Morgenstern, U.: Assessing the controls and uncertainties on mean transit times in contrasting headwater catchments, *J. Hydrol.*, 557, 16–29, doi:10.1016/j.jhydrol.2017.12.007, 2018.
- 655
- Cartwright, I. and Morgenstern, U.: Contrasting transit times of water from peatlands and eucalypt forests in the Australian Alps determined by tritium: implications for vulnerability and source of water in upland catchments, *Hydrol. Earth Syst. Sci.*, 20, 4757–4773, doi:10.5194/hess-20-4757-2016, 2016.
- Cartwright, I. and Morgenstern, U.: Transit times from rainfall to baseflow in headwater catchments estimated using tritium: the Ovens River, Australia, *Hydrol. Earth Syst. Sci.*, 19, 3771–3785, doi:10.5194/hess-19-3771-2015, 2015.
- 660
- Chen, Z., Qi, J., Xu, J., X, J., Ye, H., and Nan, Y.: Paleoclimatic interpretation of the past 30 ka from isotopic studies of the deep confined aquifer of the North China Plain, *Appl. Geochem.*, 18, 997–1009, doi:10.1016/S0883-2927(02)00206-8, 2003.
- Clark, I. D. and Fritz, P.: *Environmental Isotopes in Hydrogeology*, Lewis, New York, USA, 1997.
- Craig, H.: Isotopic variations in meteoric waters, *Science*, 133, 1702–1703, doi:10.1126/science.133.3465.1702, 1961.
- 665
- Cook, P. G., and Böhlke, J. K.: Determining timescales for groundwater flow and solute transport, in: *Environmental Tracers in Subsurface Hydrology*, Cook, P. G. and Herczeg, A. L. (Eds.), Kluwer, Boston, Netherlands, 1–30, 2000.

- Cook, P., Dogramaci, S., McCallum, J., and Hedley, J.: Groundwater age, mixing and flow rates in the vicinity of large open pit mines, Pilbara region, northwestern Australia, *Hydrogeol. J.*, 25, 39–53, doi:10.1007/s10040-016-1467-y, 2017.
- 670 Cook, P. G., Plummer, L. N., Solomon, D. K., Busenberg, E., and Han, L. F.: Effects and processes that can modify apparent CFC age, in: *Use of Chlorofluorocarbons in Hydrology: A Guidebook*, Gröning, M., Han, L. F., and Aggarwal, P. (Eds.), International Atomic Energy Agency, Vienna, Austria, 31–58, 2006.
- Cook, P. G. and Solomon, D. K.: Transport of atmospheric tracer gases to the water table: Implications for groundwater dating with chlorofluorocarbons and krypton 85, *Water Resour. Res.*, 31, 263–270, doi:10.1029/94WR02232, 1995.
- 675 Cui, W. G., Mu, G. J., Wen, Q., and Yue, J.: Evolution of alluvial fans and reaction to the regional activity at range front of Manas River Valley, *Res. Soil Water Conserv.*, 14, 161–163, 2007.
- Custodio, E., Jódar, J., Herrera, C., Custodio-Ayala, J., and Medina, A.: Changes in groundwater reserves and radiocarbon and chloride content due to a wet period intercalated in an arid climate sequence in a large unconfined aquifer, *J. Hydrol.*, 556, 427–437, doi:10.1016/j.jhydrol.2017.11.035, 2018.
- Dansgaard, W.: Stable isotopes in precipitation, *Tellus*, 16, 436–468, doi:10.1111/j.2153-3490.1964.tb00181.x, 1964.
- 680 Darling, W. G., Gooddy, D. C., MacDonald, A. M., and Morris, B. L.: The practicalities of using CFCs and SF₆ for groundwater dating and tracing, *Appl. Geochem.*, 27, 1688–1697, doi:10.1016/j.apgeochem.2012.02.005, 2012.
- Dawson, T. E. and Ehleringer, J. R.: Streamside trees do not use stream water, *Nature*, 350, 335–337, 1991.
- Dreuzy, J. R. D. and Ginn, T. R.: Residence times in subsurface hydrological systems, introduction to the Special Issue, *J. Hydrol.*, 543, 1–6, doi:10.1016/j.jhydrol.2016.11.046, 2016.
- 685 Edmunds, W. M., Ma, J., Aeschbach-Hertig, W., Kipfer, R., and Darbyshire, D. P. F.: Groundwater recharge history and hydrogeochemical evolution in the Minqin Basin, North West China, *Appl. Geochem.*, 21, 2148–2170, doi:10.1016/j.apgeochem.2006.07.016, 2006.
- Gleeson, T., Befus, K. M., Jasechko, S., Luijendijk, E., and Cardenas, M. B.: The global volume and distribution of modern groundwater, *Nat. Geosci.*, 9, 161–167, doi:10.1038/NNGEO2590, 2016.
- 690 Guo, H., Wen, D., Liu, Z., Jia, Y., and Guo, Q.: A review of high arsenic groundwater in Mainland and Taiwan, China: Distribution, characteristics and geochemical processes, *Appl. Geochem.*, 41, 196–217, doi:10.1016/j.apgeochem.2013.12.016, 2014.
- Guo, Q., Planer-Friedrich, B., Liu, M., Li, J., Zhou, C., and Wang, Y.: Arsenic and thioarsenic species in the hot springs of the Rehai magmatic geothermal system, Tengchong volcanic region, China, *Chem. Geol.*, 453, 12–20, doi:10.1016/j.chemgeo.2017.02.010, 2017.
- 695 Green, C. T., Jurgens, B. C., Zhang, Y., Starn, J. J., Singleton, M. J., and Esser, B. K.: Regional oxygen reduction and denitrification rates in groundwater from multi-model residence time distributions, San Joaquin Valley, USA, *J. Hydrol.*, 543, 155–166, doi:10.1016/j.jhydrol.2016.05.018, 2016.
- Han, D., Cao, G., McCallum, J., and Song, X.: Residence times of groundwater and nitrate transport in coastal aquifer systems: Daweijia area, northeastern China, *Sci. Total Environ.*, 538, 539–554, doi:10.1016/j.scitotenv.2015.08.036, 2015.
- 700

- Han, D., Song, X., Currell, M. J., Cao, G., Zhang, Y., and Kang, Y.: A survey of groundwater levels and hydrogeochemistry in irrigated fields in the Karamay Agricultural Development Area, northwest China: Implications for soil and groundwater salinity resulting from surface water transfer for irrigation, *J. Hydrol.*, 405, 217–234, doi:10.1016/j.jhydrol.2011.03.052, 2011.
- 705 Han, D. M., Song, X. F., Currell, M. J., and Tsujimura, M.: Using chlorofluorocarbons (CFCs) and tritium to improve conceptual model of groundwater flow in the South Coast Aquifers of Laizhou Bay, China, *Hydrol. Process.*, 26, 3614–3629, doi:10.1002/hyp.8450, 2012.
- Han, L., Hacker, P., and Gröning, M.: Residence times and age distributions of spring waters at the Semmering catchment area, Eastern Austria, as inferred from tritium, CFCs and stable isotopes, *Isot. Environ. Healt. S.*, 43, 31–50, 710 doi:10.1080/10256010601154015, 2007.
- Horneman, A., Stute, M., Schlosser, P., Smethie Jr. W., Santella, N., Ho, D. T., Mailloux, B., Gorman, E., Zheng, Y., and van Geen, A.: Degradation rates of CFC–11, CFC–12 and CFC–113 in anoxic shallow aquifers of Arai-hazar Bangladesh, *J. Contam. Hydrol.*, 97, 27–41, doi:10.1016/j.jconhyd.2007.12.001, 2008.
- Hrachowitz, M., Soulsby, C., Tetzlaff, D., Dawson, J. J. C., Dunn, S. M., and Malcolm, I. A.: Using long-term data sets to 715 understand transit times in contrasting headwater catchments, *J. Hydrol.*, 367, 237–248, doi:10.1016/j.jhydrol.2009.01.001, 2009.
- Huang, T., Pang, Z., Li, J., Xiang, Y., and Zhao, Z.: Mapping groundwater renewability using age data in the Baiyang alluvial fan, NW China, *Hydrogeol. J.*, 25, 743–755, doi:10.1007/s10040-017-1534-z, 2017.
- IAEA: <http://isohis.iaea.org/water>, last access: 27 January 2016, 2006.
- 720 Jelinowska, A., Tucholka, P., Gasse, F., and Fontes, J. C.: Mineral magnetic record of environment in Late Pleistocene and Holocene sediments, Lake Manas, Xinjiang, China, *Geophys. Res. Lett.*, 22, 953–956, doi:10.1029/95GL00708, 1995.
- Ji, L.: Using stable hydrogen and oxygen isotope to research the conversion relationship of surface water and groundwater in Manas River Basin, M.S. thesis, Shihezi University, China, 58 pp., 2016.
- Jurgens, B. C., Böhlke, J. K., and Eberts, S. M.: TracerLPM (Version 1): An Excel® workbook for interpreting groundwater 725 age distributions from environmental tracer data: U.S. Geological Survey Techniques and Methods Report 4–F3, Reston, USA, 60 pp., 2012.
- Kirchner, J. W.: Aggregation in environmental systems – Part 1: Seasonal tracer cycles quantify young water fractions, but not mean transit times, in spatially heterogeneous catchments, *Hydrol. Earth Syst. Sci.*, 20, 279–297, doi:10.5194/hess-20-279-2016, 2016.
- 730 Kirchner, J. W., Tetzlaff, D., and Soulsby C.: Comparing chloride and water isotopes as hydrological tracers in two Scottish catchments, *Hydrol. Process.*, 24, 1631–1645, doi:10.1002/hyp.7676, 2010.
- Koh, D. C., Ha, K., Lee, K. S., Yoon, Y. Y., and Ko, K. S.: Flow paths and mixing properties of groundwater using hydrogeochemistry and environmental tracers in the southwestern area of Jeju volcanic island, *J. Hydrol.*, 432–433, 61–74, doi:10.1016/j.jhydrol.2012.02.030, 2012.

- 735 Kong, Y. and Pang, Z.: A positive altitude gradient of isotopes in the precipitation over the Tianshan Mountains: Effects of moisture recycling and sub-cloud evaporation, *J. Hydrol.*, 542, 222–230, doi:10.1016/j.jhydrol.2016.09.007, 2016.
- Li, J., Pang, Z., Froehlich, K., Huang, T., Kong, Y., Song, W., and Yun, H.: Paleo-environment from isotopes and hydrochemistry of groundwater in East Junggar Basin, Northwest China, *J. Hydrol.*, 529, 650–661, doi:10.1016/j.jhydrol.2015.02.019, 2015.
- 740 Ma, B., Jin, M., Liang, X., and Li, J.: Groundwater mixing and mineralization processes in a mountain-oasis-desert basin, northwest China: hydrogeochemistry and environmental tracer indicators, *Hydrogeol. J.*, 26, 233–250, doi:10.1007/s10040-017-1659-0, 2018.
- Ma, B., Liang, X., Jin, M., Li, J., and Niu, H.: Characteristics of fractionation of hydrogen and oxygen isotopes in evaporating water in the typical region of the North China Plain, *Adv. Water Sci.*, 26, 639–648, doi:10.14042/j.cnki.32.1309.2015.05.005, 2015.
- 745 Mahlkecht, J., Hernández-Antonio, A., Eastoe, C. J., Tamez-Meléndez, C., Ledesma-Ruiz, R., Ramos-Leal, J. A., and Ornelas-Soto, N.: Understanding the dynamics and contamination of an urban aquifer system using groundwater age (^{14}C , ^3H , CFCs) and chemistry, *Hydrol. Process.*, 31, 2365–2380, doi:10.1002/hyp.11182, 2017.
- Małozzewski, P.: Lumped-parameter models as a tool for determining the hydrological parameters of some groundwater systems based on isotope data, *IAHS-AISH Publication*, 271–276, 2000.
- 750 Małozzewski, P. and Zuber, A.: Determining the turnover time of groundwater systems with the aid of environmental tracers, 1. Models and their applicability, *J. Hydrol.*, 57, 207–231, doi:10.1016/0022-1694(82)90147-0, 1982.
- McGuire, K. J. and McDonnell, J. J.: A review and evaluation of catchment transit time modeling, *J. Hydrol.*, 330, 543–563, doi:10.1016/j.jhydrol.2006.04.020, 2006.
- 755 McGuire, K. J., McDonnell, J. J., Weiler, M., Kendall, C., McGlynn, B. L., Welker, J. M., and Seibert, J.: The role of topography on catchment-scale water residence time, *Water Resour. Res.*, 41, 302–317, doi:10.1029/2004WR003657, 2005.
- Morgenstern, U. and Daughney, C. J.: Groundwater age for identification of baseline groundwater quality and impacts of land-use intensification – The National Groundwater Monitoring Programme of New Zealand, *J. Hydrol.*, 456–457, 79–760 93, doi:10.1016/j.jhydrol.2012.06.010, 2012.
- Morgenstern, U., Daughney, C. J., Leonard, G., Gordon, D., Donath, F. M., and Reeves, R.: Using groundwater age and hydrochemistry to understand sources and dynamics of nutrient contamination through the catchment into Lake Rotorua, New Zealand, *Hydrol. Earth Syst. Sci.*, 19, 803–822, doi:10.5194/hess-19-803-2015, 2015.
- Morgenstern, U., Stewart, M. K., and Stenger, R.: Dating of streamwater using tritium in a post nuclear bomb pulse world: 765 continuous variation of mean transit time with streamflow, *Hydrol. Earth Syst. Sci.*, 14, 2289–2301, doi:10.5194/hess-14-2289-2010, 2010.
- Morgenstern, U. and Taylor, C. B.: Ultra low-level tritium measurement using electrolytic enrichment and LSC, *Isot. Environ. Healt. S.*, 45, 96–117, doi:10.1080/10256010902931194, 2009.

- Négrel, P., Petelet–Giraud, E., and Millot, R.: Tracing water cycle in regulated basin using stable $\delta^2\text{H}$ – $\delta^{18}\text{O}$ isotopes: The Ebro river basin (Spain), *Chem. Geol.*, 422, 71–81, doi:10.1016/j.chemgeo.2015.12.009, 2016.
- Oster, H., Sonntag, C., and Münnich, K. O.: Groundwater age dating with chlorofluorocarbons, *Water Resour. Res.*, 32, 1989–3001, doi:10.1029/96WR01775, 1996.
- Pearson, F. J. and Hanshaw, B. B.: Sources of dissolved carbonate species in groundwater and their effects on carbon–14 dating, in: *Proceedings of A Symposium on Use of Isotopes in Hydrology*, International Atomic Energy Agency, Vienna, Austria, 271–286, 1970.
- Plummer, L. N., Busenberg, E., and Cook, P. G.: Principles of Chlorofluorocarbon dating, in: *Use of Chlorofluorocarbons in Hydrology: A Guidebook*, Gröning, M., Han, L. F., and Aggarwal, P. (Eds.), International Atomic Energy Agency, Vienna, Austria, 17–29, 2006a.
- Plummer, L. N., Busenberg, E., and Han, L. F.: CFCs in binary mixtures of young and old groundwater, in: *Use of Chlorofluorocarbons in Hydrology: A Guidebook*, Gröning, M., Han, L. F., and Aggarwal, P. (Eds.), International Atomic Energy Agency, Vienna, Austria, 59–72, 2006b.
- Polach, H. A.: Evaluation and status of liquid scintillation counting for radiocarbon dating, *Radiocarbon*, 29, 1–11, doi:10.1017/S0033822200043502, 1987.
- Qin, D.: Decline in the concentrations of chlorofluorocarbons (CFC–11, CFC–12 and CFC–113) in an urban area of Beijing, China, *Atmos. Environ.*, 41, 8424–8430, doi:10.1016/j.atmosenv.2007.07.005, 2007.
- Qin, D., Qian, Y., Han, L., Wang, Z., Li, C., and Zhao, Z.: Assessing impact of irrigation water on groundwater recharge and quality in arid environment using CFCs, tritium and stable isotopes, in the Zhangye Basin, Northwest China, *J. Hydrol.*, 405, 194–208, doi:10.1016/j.jhydrol.2011.05.023, 2011.
- Russell, A. D. and Thompson, G. M.: Mechanisms leading to enrichment of the atmospheric fluorocarbons CCl_3F and CCl_2F_2 in groundwater, *Water Resour. Res.*, 19, 57–60, doi:10.1029/WR019i001p00057, 1983.
- Stewart, M. K., Morgenstern, U., Gusyev, M. A., and Małoszewski, P.: Aggregation effects on tritium–based mean transit times and young water fractions in spatially heterogeneous catchments and groundwater systems, *Hydrol. Earth Syst. Sci.*, 21, 4615–4627, doi:10.5194/hess-21-4615-2017, 2017.
- Stewart, M. K., Morgenstern, U., and McDonnell, J. J.: Truncation of stream residence time: how the use of stable isotopes has skewed our concept of stream water age and origin, *Hydrol. Process.*, 24, 1646–1659, doi:10.1002/hyp.7576, 2010.
- Suckow, A.: The age of groundwater – Definitions, models and why we do not need this term, *App. Geochem*, 50, 222–230, doi:10.1016/j.apgeochem.2014.04.016, 2014.
- Tadros, C. V., Hughes, C. E., Crawford, J., Hollins, S. E., and Chisari, R.: Tritium in Australian precipitation: A 50 year record, *J. Hydrol.*, 513, 262–273, doi:10.1016/j.jhydrol.2014.03.031, 2014.
- Visser, A., Broers, H. P., Purtschert, R., Sültenfuß, J., and de Jonge, M.: Groundwater age distributions at a public drinking water supply well field derived from multiple age tracers (^{85}Kr , $^3\text{H}/^3\text{He}$, and ^{39}Ar), *Water Resour. Res.*, 49, 7778–7796, doi:10.1002/2013WR014012, 2013.

- Vogel, J. C.: Carbon-14 dating of groundwater, in: Proceedings of A Symposium on Use of Isotopes in Hydrology, International Atomic Energy Agency, Vienna, Austria, 225-239, 1970.
- 805 Wang, Y., Shvartsev, S. L., and Su, C.: Genesis of arsenic/fluoride-enriched soda water: A case study at Datong, northern China, *Appl. Geochem.*, 24, 641-649, doi:10.1016/j.apgeochem.2008.12.015, 2009.
- Wu, B.: Study on groundwater system evolvement law and water environment effect of Shihezi City, Ph.D. thesis, Xinjiang Agricultural University, China, 132 pp., 2007.
- Zhao, B. F.: Recharge on water resources characteristics and its rational development pattern for arid areas: a case of Manas
810 River Basin, Ph.D. thesis, Chang'an University, China, 182 pp., 2010.
- Zhou, H. C.: Groundwater system and recharge from the remote river in Southwestern margin of the Jungger Basin, Ph.D. thesis, Chinese Academy of Geological Sciences, China, 116 pp., 1992.

Table 1. Chemical–physical parameters, stable isotopes, CFC concentrations, tritium (^3H), and ^{14}C , ~~and CFC concentrations~~ in groundwater samples in the Manas River Basin.

Sample ID	Sampling date (d/m/y)	Elevation (m a.s.l.) ^a	Well depth (m)	pH	T (°C)	EC ($\mu\text{S cm}^{-1}$)	DO (mg L^{-1})	$\delta^2\text{H}$ (‰)	$\delta^{18}\text{O}$ (‰)	CFC–11 (pmol L^{-1})	CFC–12 (pmol L^{-1})	CFC–113 (pmol L^{-1})	^3H (TU)	$a^{14}\text{C}$ (pMC)	$^{14}\text{C}_{\text{eff}}$ age (years)
<i>Upstream groundwater (UG)</i>															
G1	5/6/2015	1083	170 ^b					–67.60	–10.15				41.07		
G2	5/6/2015	1107	170 ^b					–67.40	–10.17				41.13		
G3	9/8/2015	755	150	10.1	11.5	387	9.8	–70.39	–10.50	3.14	2.18	0.38			
G4	6/6/2015	532	58					–66.80	–9.91				60.04		
<i>Midstream groundwater (MG)</i>															
G5	8/8/2015	467	100	8.6	13.4	896	4.6	–69.35	–10.73	0.17	0.19	0.02	3.80		
G6	8/6/2015	472	175										28.90		
G7	7/8/2015	422	100	8.8	15.7	620	3.7	–69.87	–10.98	0.27	0.27	0.03			
G8	7/8/2015	412	90	9.3	13.6	513	2.1	–69.92	–11.08	1.99	1.21	0.18	5.00		
G9	8/8/2015	484	100	9.1	14.5	612	9.1	–74.58	–11.01	1.31	1.03	0.13	7.10		
G10	8/6/2015	463	145					–72.30	–11.05				9.09		
G11	8/6/2015	439	60					–68.50	–10.47				15.75		
G12	7/8/2015	368	260	9.3	19.0	327	6.7	–69.33	–10.73					86.9	–684
G13	4/8/2015	370	300	9.4	17.1	307	1.2	–76.20	–11.22					54.6	3158
G14	4/8/2015	370	60	9.0	13.2	556	1.4	–68.96	–10.43				1.10		
G15	5/8/2015	364	23	8.1	12.7	1650	1.0	–69.45	–9.86	0.99	0.91	0.14	7.10		
G16	5/8/2015	357	56	9.0	15.2	291	0.7	–76.59	–11.57	2.69	1.54	0.22	4.80		
G17	5/8/2015	367	280	9.8	17.2	263	2.5	–82.45	–12.19					53.2	3373
G18	6/8/2015	377	350 ^b	9.0	15.3	233	6.6	–75.97	–11.50					46.8	4432
G19	6/8/2015	381	118 ^b	9.0	15.4	309	5.2	–76.46	–11.46				6.90		

Sample ID	Sampling date (d/m/y)	Elevation (m a.s.l.) ^a	Well depth (m)	pH	T (°C)	EC (μS cm ⁻¹)	DO (mg L ⁻¹)	δ ² H (‰)	δ ¹⁸ O (‰)	CFC-11 (pmol L ⁻¹)	CFC-12 (pmol L ⁻¹)	CFC-113 (pmol L ⁻¹)	³ H (TU)	<i>a</i> ¹⁴ C (pMC)	¹⁴ C _{corr} age (years)
G20	6/8/2015	381	13	8.7	12.6	615	2.1	-74.99	-11.27	1.68	1.14	0.16	8.20		
G21	5/8/2015	424	180	8.8	15.6	378	8.0	-77.30	-11.60					43.4	5056
G22	6/6/2015	428	150					-69.72	-10.41				26.29		
G23	6/6/2015	446	70					-67.63	-9.92				37.50		
G24	8/8/2015	453	110	9.1	14.7	571	8.6	-77.35	-11.23	1.53	C ^c	C			
G25	8/8/2015	457	48	9.5	13.6	512	9.8	-77.91	-11.36	2.93	1.67	0.24			
<i>Downstream groundwater (DG)</i>															
G26	10/6/2015	348	40					-85.19	-12.11				6.91		
G27	29/7/2015	323	280	9.0	18.3	244		-79.83	-12.21					23.5	10127
G28	3/8/2015	353	45	9.0	13.2	246	8.0	-78.02	-11.47				2.90		
G29	11/6/2015	347	380					-86.39	-12.33				3.64	34.3	7001

815 ^a m a.s.l. = m above sea level. ^b Artesian well. ^c Contamination.

Table 2. Calculated results for CFC atmospheric partial pressures (pptv), fraction of post-1940 water, modern precipitation recharge year, fraction of post-1940 water, and mean residence times (EPM, DM, EPM, and EMM).

Sample ID	Atmospheric partial pressures (pptv)			Mixing post-1940 water in decimal year (F12/F113)	Fraction of post-1940 water (BM ^a , %)	modern precipitation recharge year (calendar year)			Mean residence times (F12) (years) ^b				
	CFC-11	CFC-12	CFC-113			CFC-11	CFC-12	CFC-113	EPM (1.5)	EPM (2.2)	DM (0.03)	DM (0.1)	EMM
G3	179.59	476.18	70.88	1990 2003	100 87	1982	1990	1990	19	22	39	47	16
G5	10.42	43.99	4.04	1983	12	1960	1962	1968	101	73	91	160	440
G7	18.49	68.99	6.85	1985	18	1963	1965	1971	89	66	82	139	270
G8	122.11	280.24	36.42	1988	64	1976	1978	1984	43	39	52	71	49
G9	85.03	251.10	27.96	1985	66	1973	1977	1982	47	42	54	76	58
G15	58.15	202.68	26.99	1988	45	1970	1974	1981	55	47	59	86	77
G16	177.81	380.91	48.36	1987	89	1982	1985	1986	30	31	45	57	29
G20	100.11	257.11	31.36	1987	62	1974	1977	1983	45	41	54	75	56
G24	99.90					1974							
G25	180.79	388.92	48.83	1985	91	1982	1986	1986	30	30	44	56	28

^a BM=binary mixing, assuming a mixture of old water with young water (post-1940). ^b Lumped parameter models: DM=dispersion model with D_p (in Eq. (3)) of 0.1 and 0.03, EPM=exponential-piston flow model with η (in Eq. (2)) of 2.2 and 1.5, EMM=exponential mixing model. F12 is short for CFC-12.

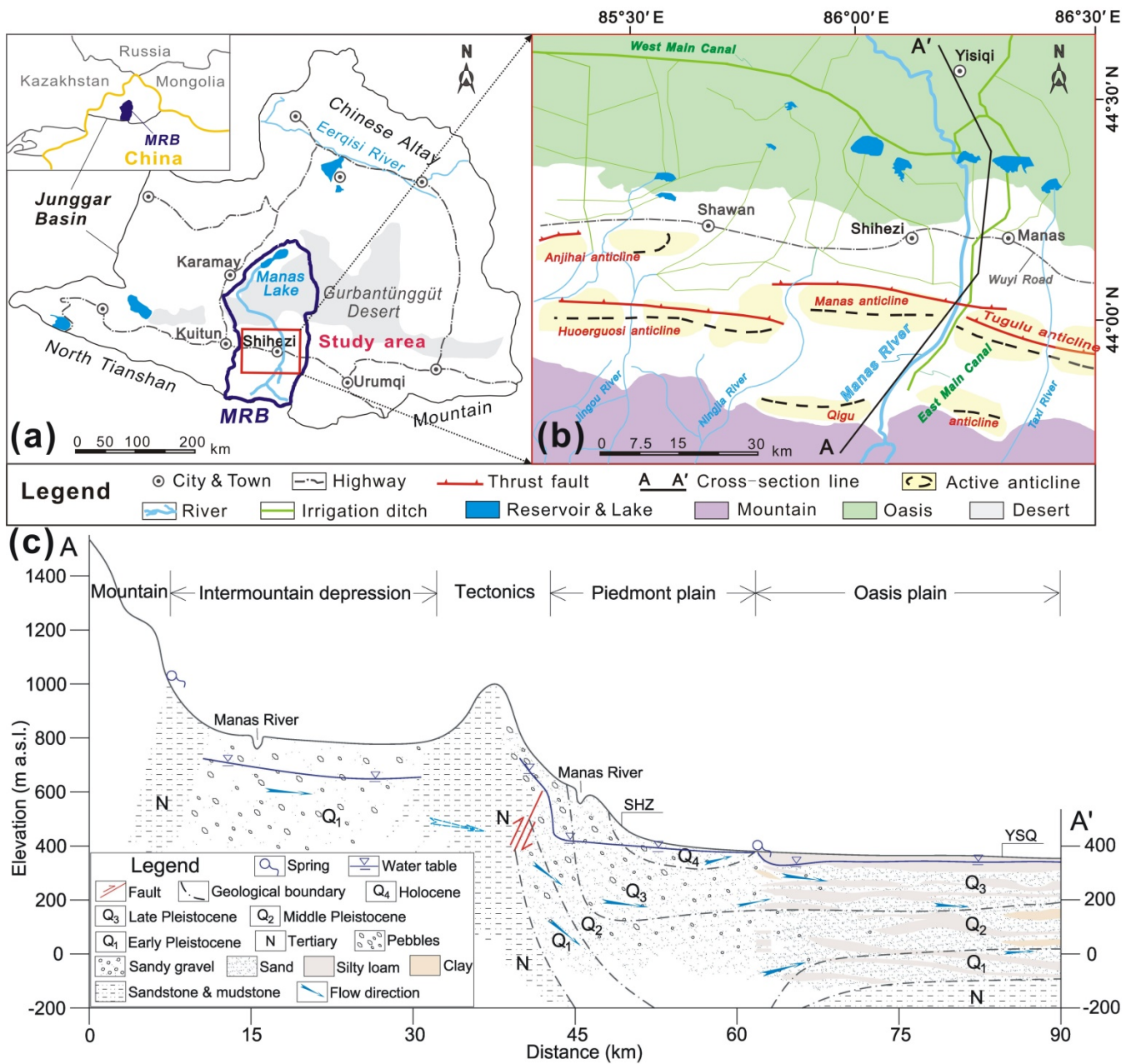


Figure 1. Maps showing (a) regional location of the Manas River Basin (modified after Ma et al., 2018), (b) surface water (river, reservoir and irrigation ditch) system (modified after Cui et al, (2007) and Ji, (2016)) and (c) geological cross-section of the study area for A–A' line shown in (b).

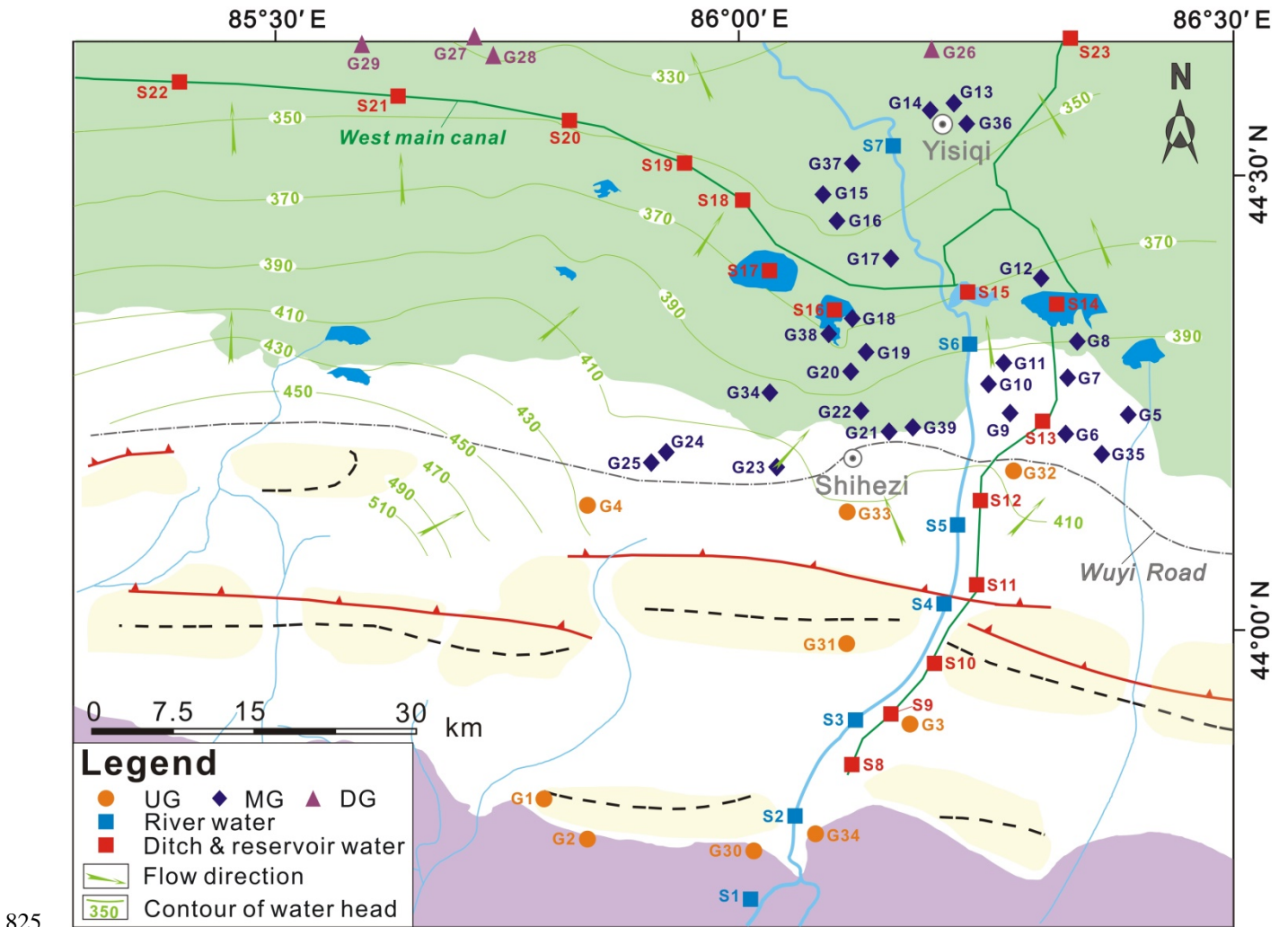
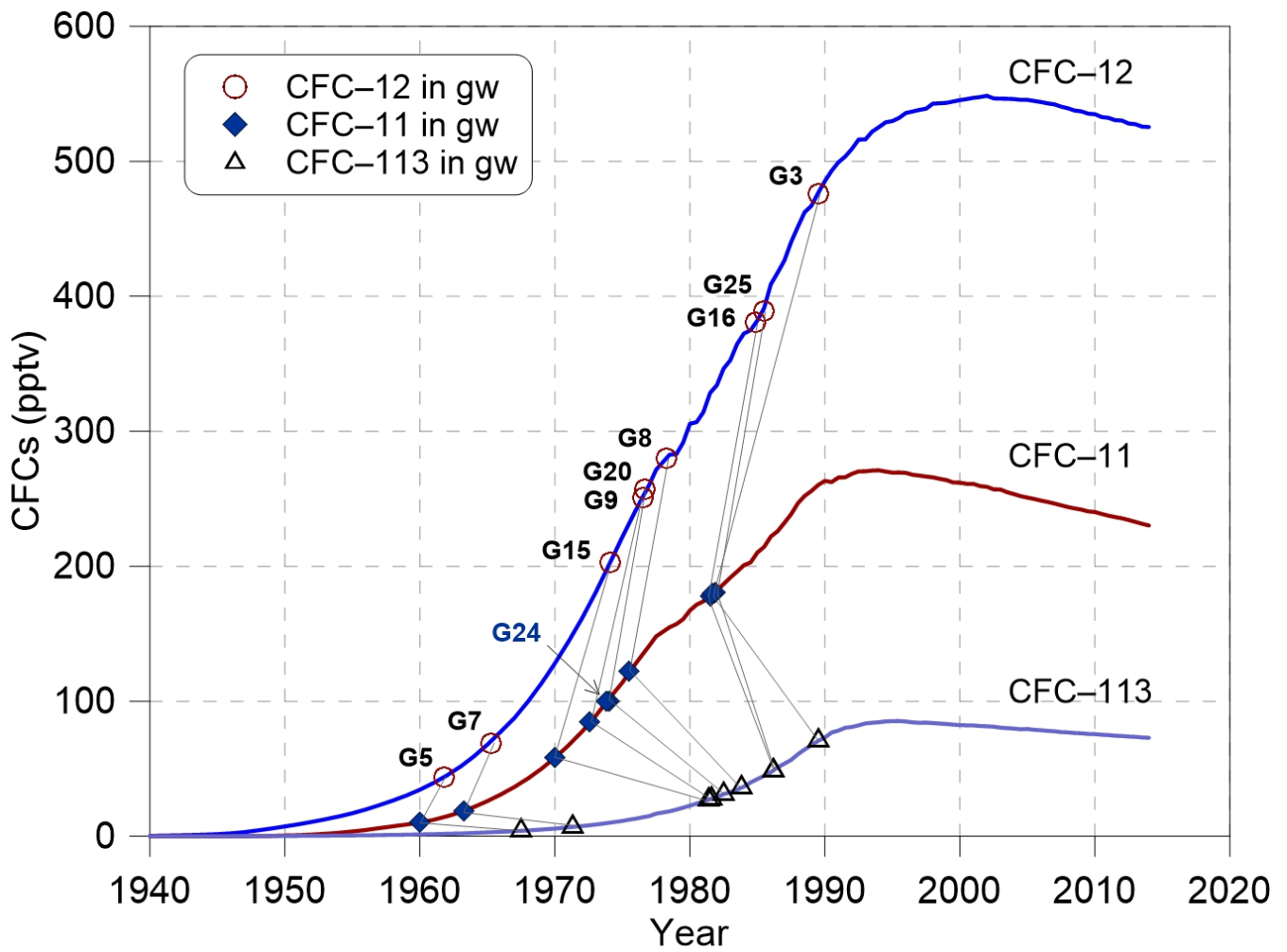


Figure 2. Water sampling sites and unconfined groundwater head contours (in meters) in the headwater catchments of Manas River. UG=Upstream Groundwater, MG=Midstream Groundwater, DG=Downstream Groundwater.



830

Figure 3. Concentrations of CFC-11, CFC-12 and CFC-113 (pptv) in the groundwater of this study area sampled in 2015 compared with the time series trend of Northern Hemisphere atmospheric mixing ratio at a recharge temperature of 10 °C. Data is available at < <http://water.usgs.gov/lab/software/air/cure/>>.

835

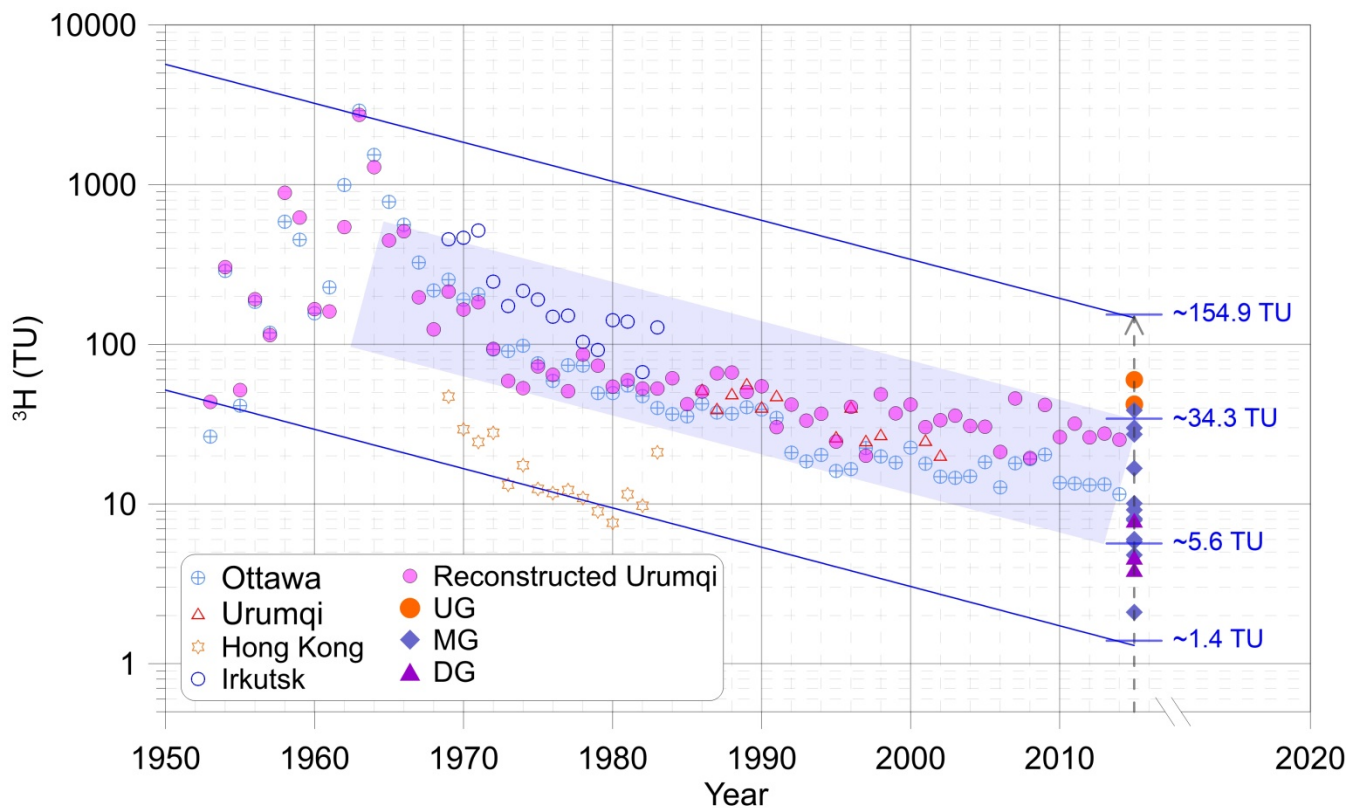
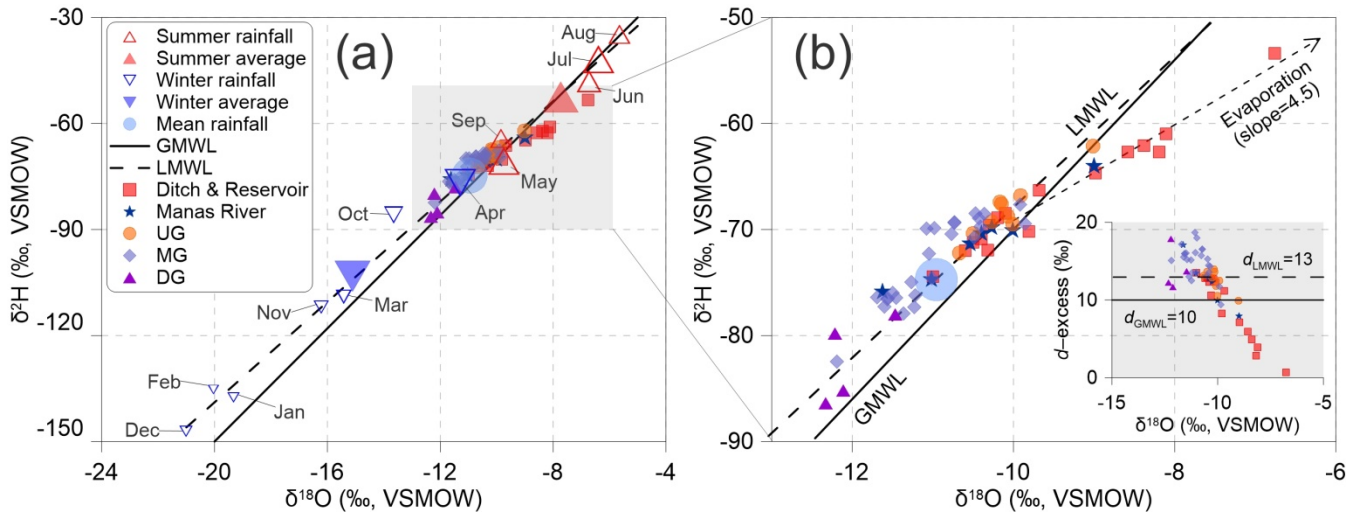


Figure 4. Tritium concentration (TU) of the upstream groundwater (UG), midstream groundwater (MG), and downstream groundwater (DG). Time series of tritium concentration in precipitation at Ottawa, Urumqi, Hong Kong, and Irkutsk were obtained by GNIP in IAEA (<https://www.iaea.org/>). The blue solid lines and shaded field were drawn using the half-life 840 (12.32 yrs) of tritium decayed to 2014.



845 **Figure 5.** (a) Plot of stable isotopes of surface water and groundwater from the mountain to the oasis plain as compared to
 the global meteoric water line (GMWL; Craig, 1961) and the local meteoric water line (LMWL, rainfall in Urumqi station of
 IAEA networks during 1986 and 2003; IAEA, 2006). The size of the hollow triangles stands for the relative amount of
 precipitation. “Mean rainfall” refers to the annual amount-weighted mean rainfall isotopic value. (b) Plot of $\delta^2\text{H}$ vs. $\delta^{18}\text{O}$
 and inserted plot d -excess vs. $\delta^{18}\text{O}$. UG=Upstream Groundwater, MG=Midstream Groundwater, DG=Downstream
 850 Groundwater.

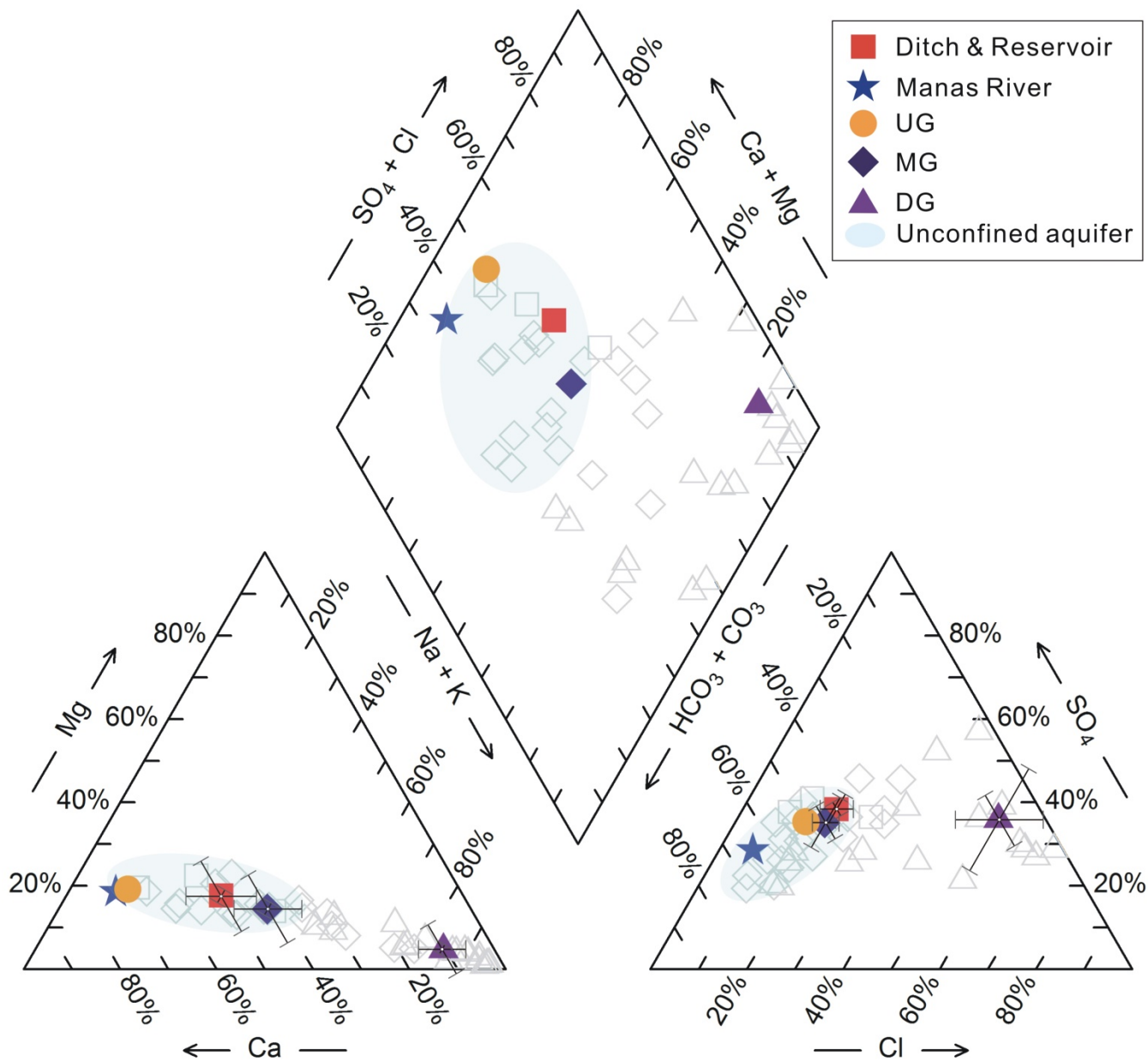


Figure 6. Piper diagram highlights the $\text{HCO}_3\text{-SO}_4\text{-Na}$ type of waters. The coloured symbols represent the mean values calculated from the hydrochemistry data (light grey hollow symbols) reported by Ma et al. (2018). The error bars are shown in the cation and anion diagrams.

855

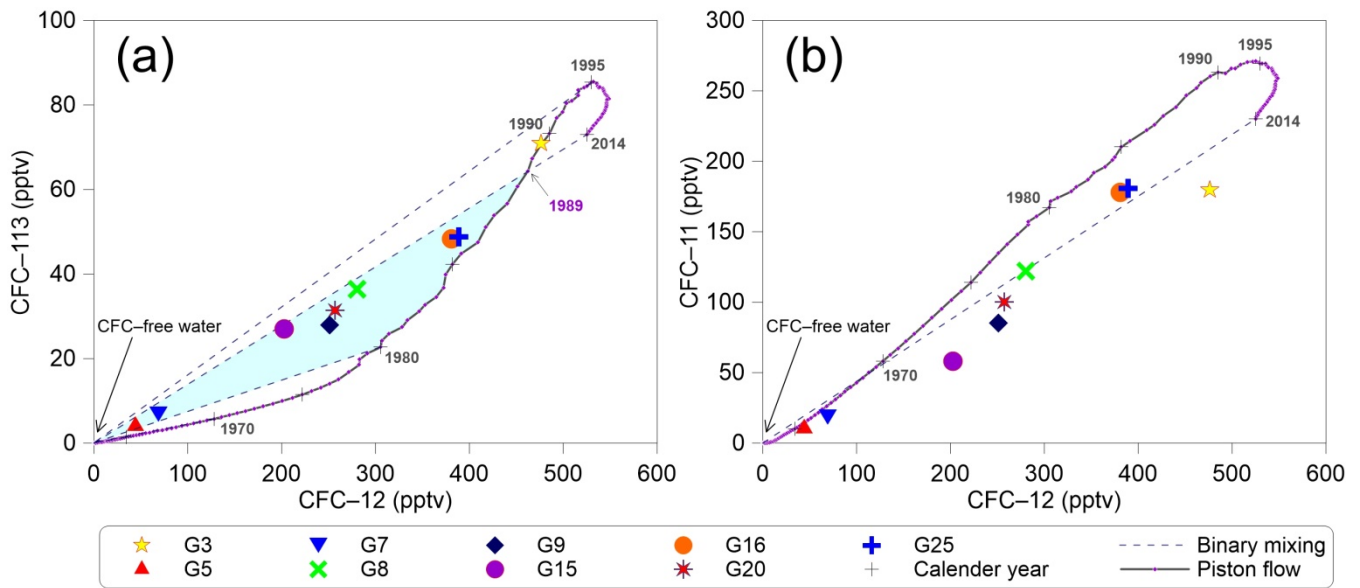


Figure 7. Plots showing relationships of (a) CFC-113 vs. CFC-12 and (b) CFC-11 vs. CFC-12 in pptv for the Northern Hemisphere air. The '+' denotes selected calendar years. The solid lines correspond to the piston flow and the short-dashed lines show the binary mixing. The shaded regions in (a) indicate no post-1989 waters mixing.

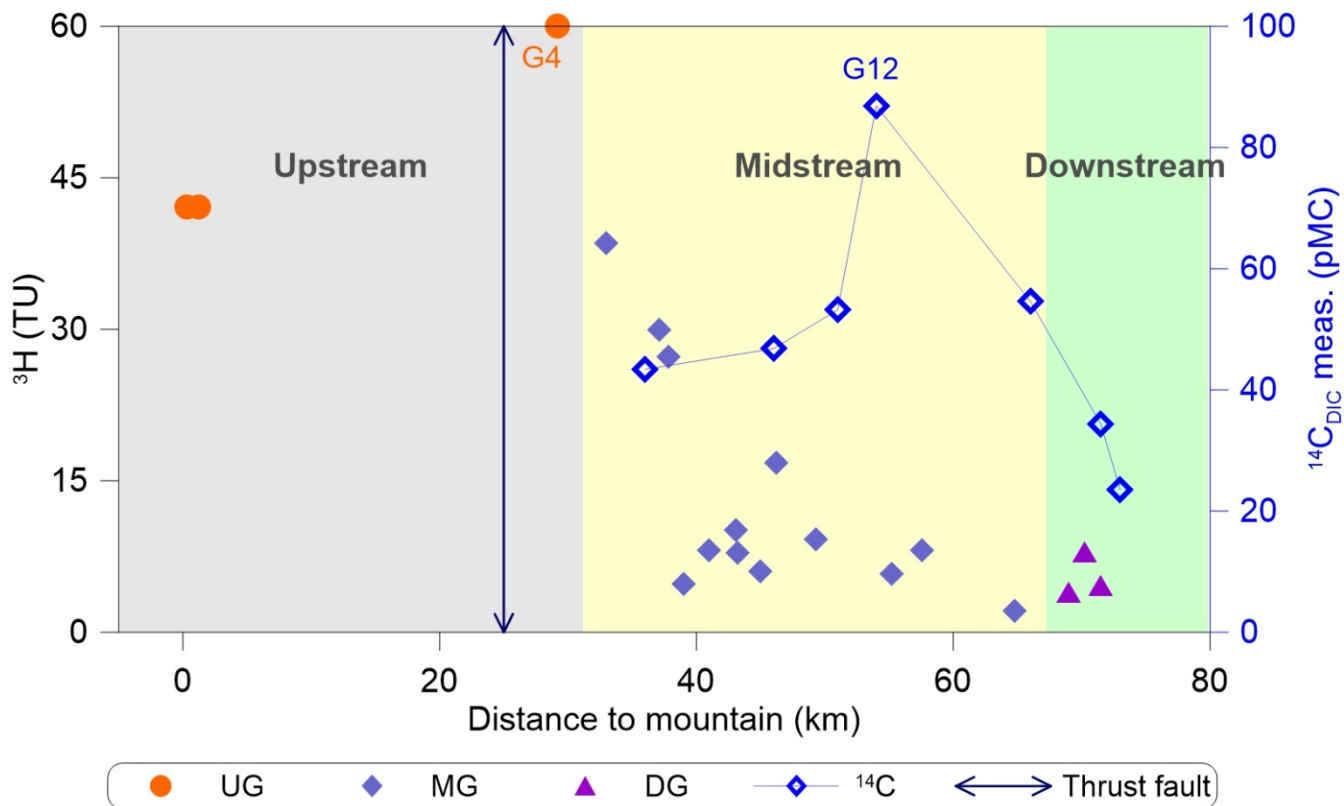


Figure 8. Distributions of ^3H and ^{14}C activities with distance to mountain. The shaded regions indicate the upstream, midstream and downstream of Manas River.

865

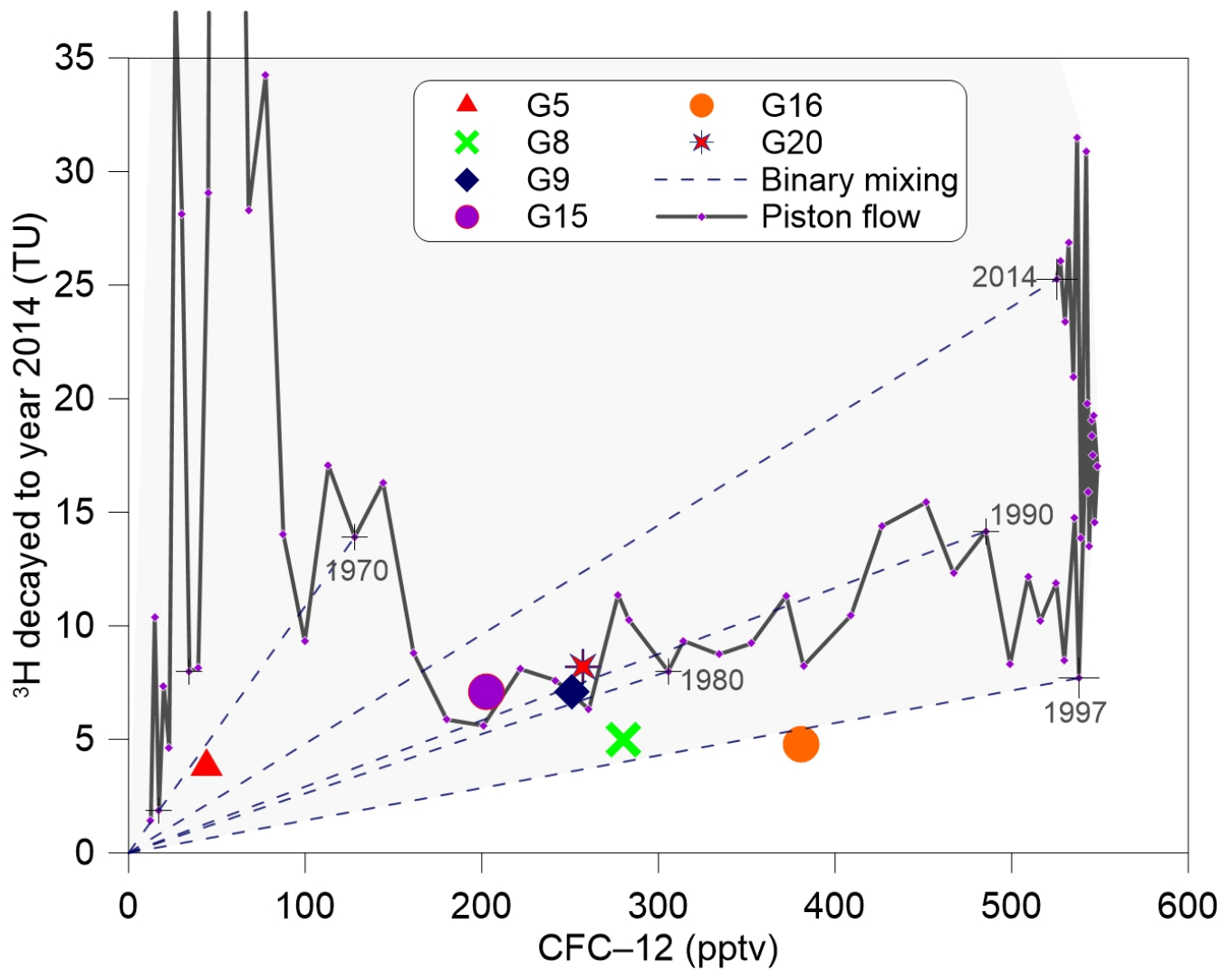


Figure 9. ^3H activity (TU) in Urumqi precipitation decayed to 2014 vs. CFC-12 in pptv for Northern Hemisphere air. The '+' denotes selected calendar years. The solid lines correspond to the piston flow and the short-dashed lines show the binary mixing. The shaded region indicates concentrations that could arise due to mixing water of different ages.

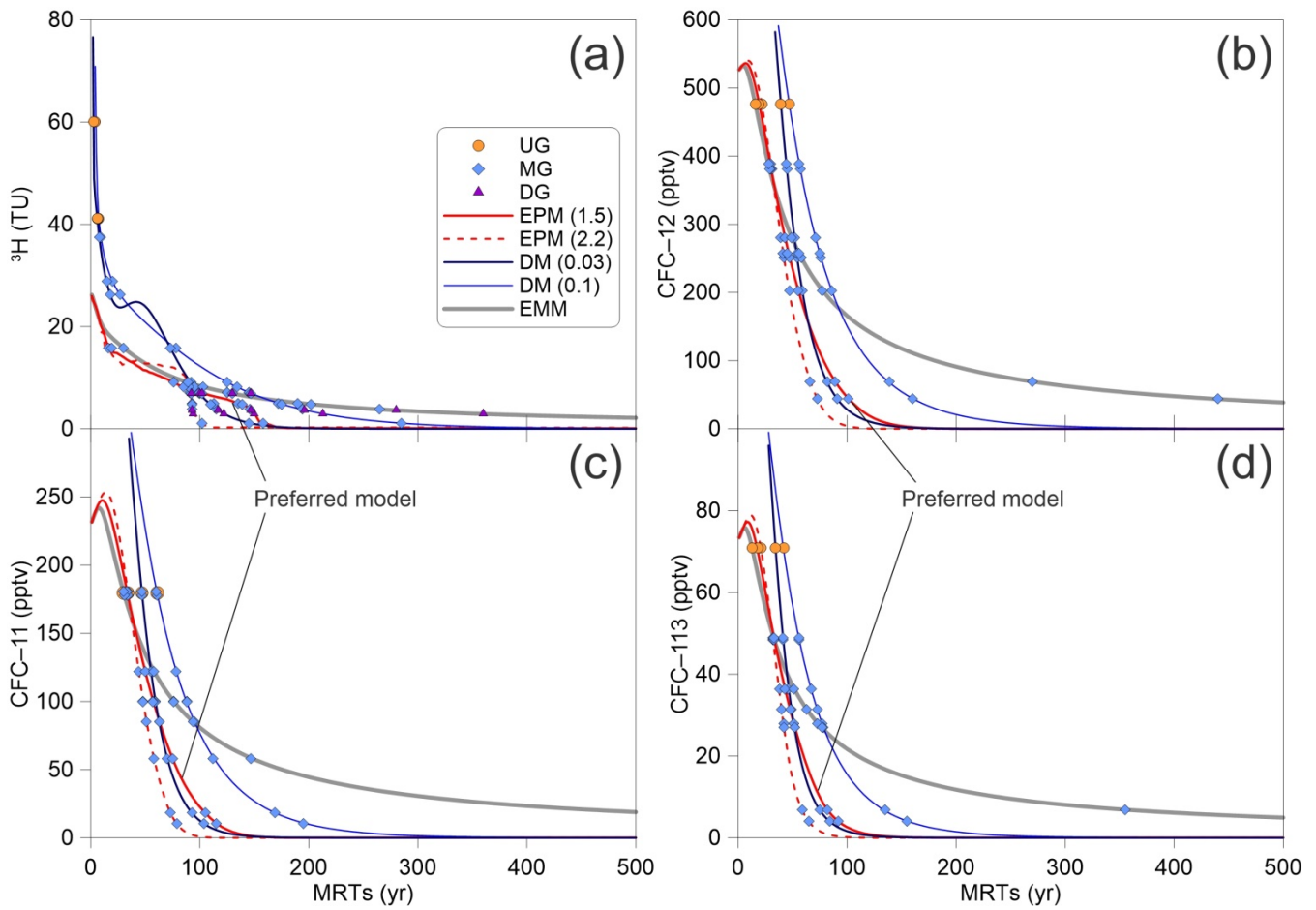


Figure 10. Tritium and CFCs (CFC-11, CFC-12 and CFC-113) output vs. mean residence times for different lumped-parameter models estimated using Eqs. (2) to (5). The input ^3H activity and CFCs concentration are using the estimated ^3H activity in precipitation in Urumqi station (Fig. 4) and the Northern Hemisphere atmospheric mixing ratio (Fig. 3),

875 respectively.

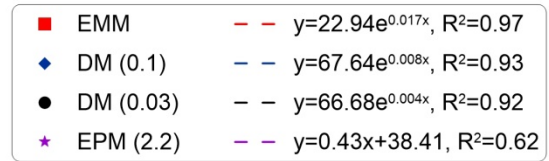
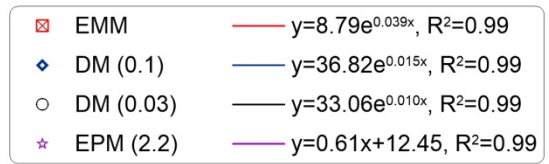
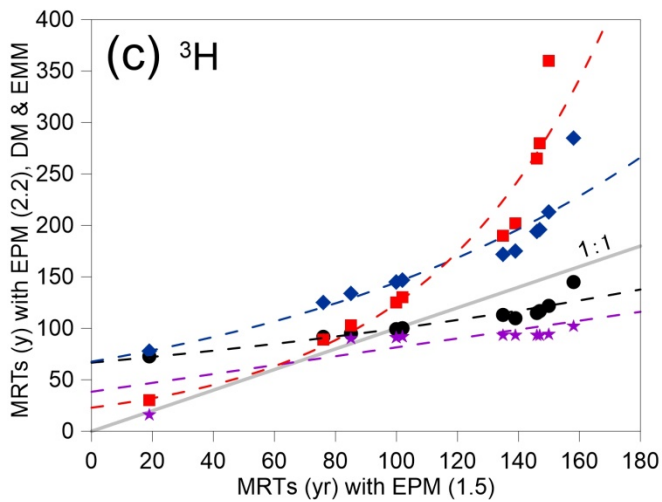
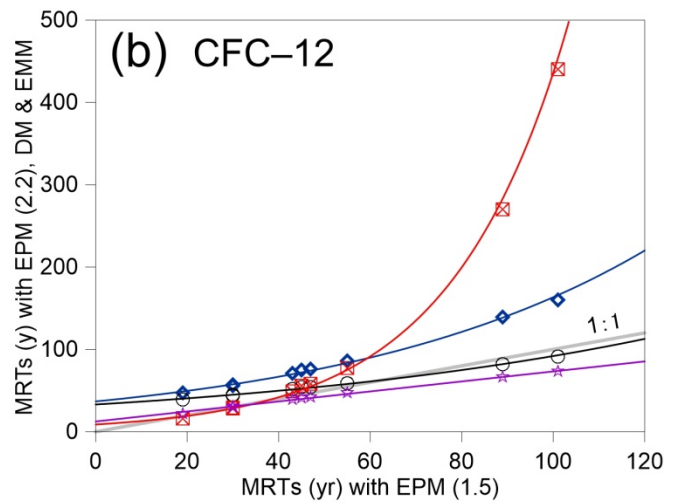
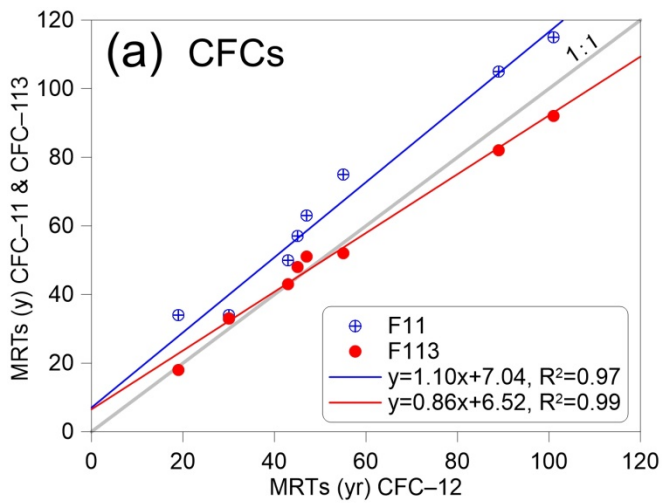


Figure 11. (a) MRTs with EPM (1.5) of CFC-12 vs. CFC-11 & CFC-113; Mean residence times (MRTs) for CFC-12 vs. MRTs for CFC-11 and CFC-113 data using the EPM (1.5) model. (b) CFC-12 MRTs with EPM (1.5) vs. EPM (2.2), DM & EMM, and MRTs for CFC-12 with EPM (1.5) vs. those with other models. (c) ³H MRTs with EPM (1.5) vs. EPM (2.2), DM & EMM MRTs for ³H vs. those with other models.

880

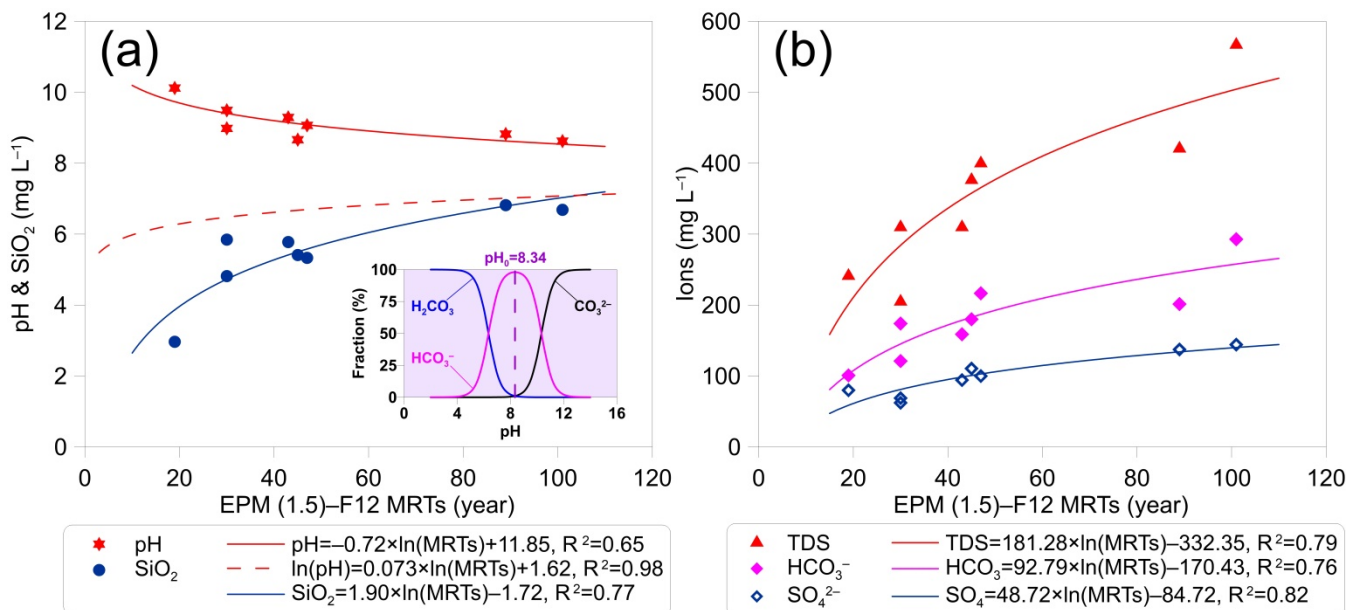


Figure 12. (a) pH & silica (SiO₂) and (b) ions including sulfate (SO₄²⁻), bicarbonate (HCO₃⁻), and total dissolved solids (TDS) vs. mean residence times (MRTs) EPM (1.5) F12 MRTs (CFC 12 MRTs using EPM (1.5)). The MRTs are from CFC-12 data using the EPM (1.5) model. The dashed red line in (a) is from Morgenstern et al. (2015).